



## ORIGINAL ARTICLE

# An insight into the vicarious nucleophilic substitution reaction of 2-nitro-5,10,15,20-tetraphenylporphyrin with *p*-chlorophenoxyacetonitrile: Synthesis and gas-phase fragmentation studies



Mohammed Eddahmi<sup>a,b</sup>, Nuno M.M. Moura<sup>b,\*</sup>, Catarina I.V. Ramos<sup>b,\*</sup>,  
Latifa Bouissane<sup>a</sup>, Maria A.F. Faustino<sup>b</sup>, José A.S. Cavaleiro<sup>b,\*</sup>,  
El Mostapha Rakib<sup>a,\*</sup>, Maria G.P.M.S. Neves<sup>b,\*</sup>

<sup>a</sup> *Laboratory of Organic and Analytic Chemistry, Faculty of Sciences and Technics, Sultan Moulay Slimane University, BP 523, 2300 Beni-Mellal, Morocco*

<sup>b</sup> *LAQV-REQUIMTE, Department of Chemistry, University of Aveiro, 3810-193 Aveiro, Portugal*

Received 3 February 2020; accepted 18 April 2020

Available online 1 May 2020

## KEYWORDS

Porphyrin;  
Vicarious nucleophilic substitution;  
ESI-MS;  
Diagnostic fragment ions

This publication is dedicated to Professor Sultan T. Abu-Orabi on the occasion of his 70th anniversary.

**Abstract** *Meso*-tetraarylporphyrins bearing nitro groups are considered as excellent templates to introduce new functionalities in the porphyrin core, namely through reactions with nucleophiles. Here the reaction of 2-nitro-5,10,15,20-tetraphenylporphyrin with *p*-chlorophenoxyacetonitrile was revisited and it was found that the reaction profile was strongly dependent on the presence or absence of a metal ion in the porphyrinic inner core and on the solvent used. Under the studied synthetic conditions several porphyrins modified at neighbouring  $\beta$ -positions with nitro, amino, ether, ester, nitrile, methylcyano and formyl functionalities were isolated. Most of them are suitable for further modifications and/or conjugation to other substrates or materials. The gas-phase fragmentation studies corroborated the proposed structures. In general, the formation of the main fragment ions involves intramolecular cyclization processes with the formation of five or six-membered rings between the  $\beta$ -pyrrolic and the *ortho* position of the adjacent *meso*-phenyl group.

© 2020 The Authors. Published by Elsevier B.V. on behalf of King Saud University. This is an open access article under the CC BY-NC-ND license (<http://creativecommons.org/licenses/by-nc-nd/4.0/>).

\* Corresponding authors.

E-mail addresses: [nmoura@ua.pt](mailto:nmoura@ua.pt) (N.M.M. Moura), [c.ramos@ua.pt](mailto:c.ramos@ua.pt) (C.I.V. Ramos), [faustino@ua.pt](mailto:faustino@ua.pt) (M.A.F. Faustino), [jcavaleiro@ua.pt](mailto:jcavaleiro@ua.pt) (J.A.S. Cavaleiro), [e.rakib@usms.ma](mailto:e.rakib@usms.ma) (E. Mostapha Rakib), [gneves@ua.pt](mailto:gneves@ua.pt) (M.G.P.M.S. Neves).

Peer review under responsibility of King Saud University.



Production and hosting by Elsevier

## 1. Introduction

Porphyrins and related macrocycles are a versatile family of aromatic compounds with a unique set of physico-chemical properties with potential application in a wide array of fields (Kadish et al., 2010), such as, medicine (Chang et al., 2016; Calvete et al., 2017; Hamblin and Abrahamse, 2018; Imran et al., 2018; Jenni and Sour, 2019; Keane and Kelly, 2018; McKenzie et al., 2019; Mesquita, et al., 2018; Sandland, et al., 2018), supramolecular chemistry (Cen et al., 2018; Kc and D'Souza, 2016; Otsuki, 2018; Rajora et al., 2017; Zheng et al., 2018), (photo)catalysis (Costentin et al., 2015; Nakagaki et al., 2016; Neves et al., 2019; Pegis et al., 2018; Zhang et al., 2017), solar cells (Di Carlo et al., 2018; Di Carlo et al. 2019; Higashino and Imahori, 2015; Kundu and Patra, 2017; Song et al., 2018; Urbani et al., 2014; Vamsi et al., 2017), electronic devices (Auwärter et al., 2015; Jurow et al., 2010; Mukhopadhyay et al., 2018; Niu and Li, 2013) and (chemo)sensors (Ding et al., 2017; El Abiad et al., 2019; Li, Yin, & Huo, 2016; Moura et al., 2014a; Moura et al., 2014b; Paolesse et al., 2017; Radi et al., 2019).

*Meso*-tetraarylporphyrins bearing primary groups (e.g. formyl, nitro) at *meso*- or  $\beta$ -positions are excellent templates to modify the substituents present in the porphyrinic macrocycle (Cerqueira et al., 2017; Cavaleiro et al., 2010; Serra et al., 2014). In particular,  $\beta$ -nitro-*meso*-tetraarylporphyrins can be used in different synthetic approaches like nucleophilic or electrophilic substitutions, nucleophilic addition, cycloaddition reactions and reduction (Serra et al., 2014). The functionalization of  $\beta$ -nitro-*meso*-tetraarylporphyrins with nucleophiles is dependent of different reaction parameters, such as temperature, solvent, nucleophile, electronic environment on the porphyrinic core and metal ion coordination. In the presence of “hard” nucleophiles, products from the attack at the pyrrolic carbon adjacent to the nitro group ( $\alpha$ -attack) are obtained, while the reaction with “soft” nucleophiles affords products from the attack at the carbon linked to the nitro group (ipso attack) (Jaquinod, 2000; Serra et al., 2014).

Smith and co-workers (Gros et al., 1997; Jaquinod et al., 1996; Jaquinod et al., 1997), described for the first time the synthesis of  $\beta$ -fused pyrroloporphyrins through a Barton-Zard condensation involving the reaction of metallo complexes of 2-nitro-5,10,15,20-tetraarylporphyrin ( $\beta$ -NO<sub>2</sub>TPP, **1**) with  $\alpha$ -isocyanoacetic ester (CNCH<sub>2</sub>CO<sub>2</sub>Et) as the nucleophilic precursor in the presence of DBU. In these studies, the Zn(II) complexes of  $\beta$ -nitro-*meso*-tetraarylporphyrins were used and gave rise to the preparation of cyclopropyl-annulated chlorins.

In 1996, Malinovskii *et al.* (Malinovskii et al., 1996) described the reaction of 2-nitro-5,10,15,20-tetraarylporphyrin, and of its Cu(II) and Zn(II) complexes with tosylmethyl bromide using KOH as base. The formation of derivatives obtained with the tosylmethyl moiety linked at the  $\beta$ -pyrrolic position adjacent to the nitro unit, was justified by considering the vicarious nucleophilic substitution (VNS) of the hydrogen in that  $\beta$ -position (Ishkov, 1999; Malinovskii et al., 1996). Thereafter, Ostrowski *et al.* (Ostrowski and Raczko, 2005) described the reaction of the Zn(II) complex of 2-nitro-5,10,15,20-tetraarylporphyrin with different carbanions generated in the presence of *t*-BuOK in DMSO, at room temperature, from the adequate aryl sulfones, a sulfon-

amide, a nitrile, an ester and a sulfane (Scheme 1). In these studies, the authors were able to isolate the products resulting just from the  $\alpha$ -attack in good to excellent yields (51–83%) from the sulfones, sulfonamide and the nitrile, and in poor yields from the reactions with the ester and sulfane (Ostrowski & Raczko, 2005). In 2017, Sankar and co-workers (Chaudri et al., 2017) reported a facile and interesting access to new porphyrins and chlorins through nucleophilic substitution of  $\beta$ -nitro-*meso*-tetraphenylporphyrin derivatives with active methylene compounds, such as cyclic 1,3-diones and benzoylacetoneitrile.

In 2017, Ostrowski *et al.* studied the reactivity of the Zn(II) and Cu(II) complexes of 5-(4-nitrophenyl)-10,15,20-triphenyl porphyrin complexes with trihalomethyl carbanions (Ostrowski et al., 2017). The products resulting from the reaction in the 4-nitrophenyl unit at the ortho position of the nitro group were isolated in yields ranging from moderate to excellent (32–87%); the authors commented that these VNS reactions must be performed at low temperatures (–70 to –78 °C) in order to avoid the decomposition of the carbanions (Ostrowski et al., 2017). The VNS approach had been previously explored by the same group to prepare free-base porphyrins with *meso*-aryl units highly substituted from adequate *meso*-nitrophenylporphyrins (Ostrowski et al. 2003; Ostrowski et al. 2004).

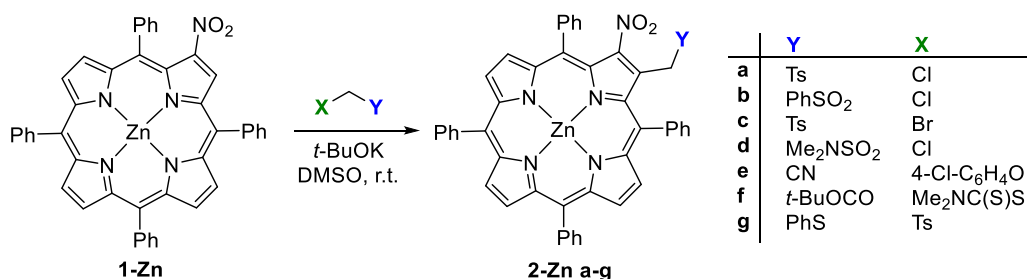
Following our interest into the  $\beta$ -modification of *meso*-tetraarylporphyrins, (Amiri et al., 2019; Linhares et al., 2014; Pereira et al., 2008; Pereira et al., 2014; Rebelo et al., 2004; Rebelo et al. 2005; Rebelo et al., 2006; Soares et al., 2007) we decided to revisit the VNS reaction of *p*-chlorophenoxyacetoneitrile but using the free-base 2-nitro-5,10,15,20-tetraarylporphyrin **1**. According with literature (Ostrowski & Raczko, 2005), it was expected in this reaction to obtain directly the free-base of **2-Zne** (Scheme 1) from now on referred as compound **2**, resulting from the cyanomethylation at the  $\beta$ -pyrrolic carbon adjacent to the nitro unit. It was expected that the introduction of that functionality at the  $\beta$ -pyrrolic position adjacent to the nitro group could allow further modifications leading to chlorins with improved absorption in the therapeutic window, to introduce target molecules for cancer cells (e.g. sugar units, antibodies) through Knoevenagel and alkylation reactions (Eddahmi et al., 2019a) and also to be explored as anion sensing due to the acidity of the CH<sub>2</sub>CN chain (Eddahmi et al., 2019b).

To our surprise, the absence of a metal ion in the inner core of the macrocycle gave rise to a different reaction profile, and the results achieved encouraged us to explore different reaction conditions using either the free base  $\beta$ -NO<sub>2</sub>TPP or their Zn(II) and Cu(II) complexes. Additionally, the gas-phase fragmentation pattern of the new derivatives was evaluated by ESI-MS (electrospray mass spectrometry) in order to corroborate the proposed structures.

## 2. Materials and methods

### 2.1. General remarks

<sup>1</sup>H and <sup>13</sup>C NMR spectra were recorded on Bruker Avance 500 (500.13 and 125.47 MHz, respectively) spectrometer. CDCl<sub>3</sub> was used as solvent and tetramethylsilane (TMS) as



**Scheme 1** Vicarious nucleophilic substitution (VNS) between Zn(II) complex of  $\beta$ -NO<sub>2</sub>TPP with a series of carbanions reported by Ostrowski *et al.* (Ostrowski & Raczko, 2005).

the internal reference; the chemical shifts are expressed in  $\delta$  (ppm) and the coupling constants ( $J$ ) in Hertz (Hz).

Unequivocal <sup>1</sup>H assignments were made using 2D COSY (<sup>1</sup>H/<sup>1</sup>H). Preparative thin-layer chromatography was carried out on 20 × 20 cm glass plates coated with silica gel (0.5 mm thick). Column chromatography was carried out using silica gel (Merck, 35–70 mesh). Analytical TLC was carried out on precoated sheets with silica gel (Merck 60, 0.2 mm thick). The absorption spectra (see Fig. S28) were recorded on a UV-2501PC Shimadzu spectrophotometer using DMF as solvent. The studied solutions were prepared by appropriate dilution up to 10<sup>-5</sup>–10<sup>-6</sup> M of the stock solutions. All the measurements were performed at 298 K.

## 2.2. Chemicals

All chemicals were used as supplied. Solvents were used as received or distilled and dried using standard procedures according to the literature procedures (Armarego and Chai, 2013). The starting reagent, 2-nitro-5,10,15,20-tetraphenylporphyrin **1**, was prepared from 5,10,15,20-tetraphenylporphyrin, copper nitrate, acetic acid, anhydride acetic in chloroform, according to a published procedure (Alonso *et al.*, 2005; Baldwin *et al.*, 1982). The structure of the synthesized compound **1** was confirmed by <sup>1</sup>H NMR spectroscopic and mass spectrometry data.

## 2.3. Reactions of *p*-chlorophenoxyacetonitrile with 2-nitro-5,10,15,20-tetraphenylporphyrin

In here are only described the procedures that allowed to isolate the new derivatives in better yields. The results obtained using other experimental conditions tested are summarized in Table S1.

### 2.3.1. Synthesis of compound 3

To a solution of  $\beta$ -NO<sub>2</sub>TPP **1** (20 mg, 0.03 mmol) in toluene (2 mL) was added *t*-BuOK (17 mg, 0.3 mmol) and *p*-chlorophenoxyacetonitrile (25 mg, 0.15 mmol). The mixture was stirred at 110 °C in an oil bath for 72 h when the TLC control showed the complete consumption of the starting porphyrin. After cooling, the reaction mixture was washed with water, extracted with dichloromethane and the organic phase was dried (Na<sub>2</sub>SO<sub>4</sub>) and the solvent was evaporated under reduced pressure. The crude mixture was purified by preparative thin-layer chromatography using toluene

as eluent affording compound **3** as the major product in 28% yield.

**2.3.1.1. 2-amino-3-nitro-5,10,15,20-tetraphenylporphyrin, 3.** **Yield:** 28% (5.7 mg, 8.5  $\mu$ mol). **<sup>1</sup>H NMR** (500 MHz, CDCl<sub>3</sub>):  $\delta$  8.95 (1H, d,  $J$  = 5.0 Hz, H- $\beta$ ), 8.77 (1H, d,  $J$  = 5.0 Hz, H- $\beta$ ), 8.75 (1H, d,  $J$  = 4.8 Hz, H- $\beta$ ), 8.24–8.15 (2H, m, H- $\beta$ ), 8.58 (1H, d,  $J$  = 4.8 Hz, H- $\beta$ ), 8.35 (2H, d,  $J$  = 7.7 Hz, H-*o*-Ph), 8.24–8.15 (6H, m, H-*o*-Ph), 7.94–7.88 (3H, m, H-*p*-Ph), 7.81–7.69 (8H, m, H-*m*-Ph), 7.49 (1H, t,  $J$  = 7.2 Hz, H-*p*-Ph), 6.80 (2H, s, NH<sub>2</sub>), –2.33 (1H, s, N-H), –2.57 (1H, s, N-H) ppm. **<sup>13</sup>C NMR** (125 MHz, CDCl<sub>3</sub>):  $\delta$  156.4, 155.1, 154.5, 148.0, 142.1, 141.51, 141.45, 140.2, 139.6, 139.3, 138.1, 137.7, 135.2, 135.0, 134.5, 134.1, 133.1, 129.7, 129.6, 129.3, 129.2, 128.9, 128.00, 127.97, 127.7, 127.33, 127.31, 127.2, 127.0, 126.9, 122.0, 120.4, 118.2, 117.2, 116.7 ppm. **UV-Vis** (DMF):  $\lambda_{\max}$  ( $\epsilon$ ) 432 (106045), 531 (7285.1), 567 (4952.8), 608 (2886.4), 668 (1684.2) nm (cm<sup>-1</sup> M<sup>-1</sup>). **MS-ESI(+):**  $m/z$  calculated for C<sub>44</sub>H<sub>31</sub>N<sub>6</sub>O<sub>2</sub> 675.25 [M+H]<sup>+</sup> and 338.13 [M+2H]<sup>2+</sup>; found  $m/z$  675.35 and  $m/z$  338.21

### 2.3.2. Synthesis of compound 4

To a solution of  $\beta$ -NO<sub>2</sub>TPP **1** (20 mg, 0.03 mmol) in *N,N*-dimethylformamide (DMF) (2 mL) was added *t*-BuOK (17 mg, 0.3 mmol) and *p*-chlorophenoxyacetonitrile (25 mg, 0.15 mmol). The mixture was stirred at 60 °C in an oil bath for 24 h and monitored by TLC. After cooling, the reaction was washed with water, extracted with dichloromethane and the organic phase was dried (Na<sub>2</sub>SO<sub>4</sub>) and the solvent was evaporated under reduced pressure. The crude mixture was purified by preparative thin-layer chromatography using toluene as eluent affording compound **4** as the major product in 34% yield).

When the reaction was performed in DMSO under the same conditions compound **4** was isolated in 23%.

**2.3.2.1. 2-carbonitrile-3-(4-chlorophenoxy)-5,10,15,20-tetraphenylporphyrin, 4.** **Yield:** in DMF – 23% (4.9 mg, 6.4  $\mu$ mol); in DMSO – 34% (7.2 mg, 9.4  $\mu$ mol) in DMSO. **<sup>1</sup>H NMR** (500 MHz, CDCl<sub>3</sub>):  $\delta$  8.92 (2H, s, H- $\beta$ ), 8.86 (1H, d,  $J$  = 5.0 Hz, H- $\beta$ ), 8.77 (1H, d,  $J$  = 5.0 Hz, H- $\beta$ ), 8.74–8.71 (2H, m, H- $\beta$ ), 8.23–8.15 (6H, m, H-*o*-Ph), 7.91 (2H, d,  $J$  = 7.3 Hz, H-*o*-Ph), 7.86 (1H, t,  $J$  = 7.3 Hz, H-*p*-Ph), 7.81–7.72 (8H, m, H-*m*-Ph), 7.58 (1H, t,  $J$  = 7.6 Hz, H-*p*-Ph), 7.50 (1H, t,  $J$  = 7.3 Hz, H-*p*-Ph), 7.04 (2H, d,  $J$  = 9.0 Hz, H-3,5), 6.57 (2H, d,  $J$  = 9.0 Hz, H-2,6), –2.80

(2H, s, *N*-H) ppm.  $^{13}\text{C}$  NMR (125 MHz,  $\text{CDCl}_3$ ):  $\delta$  156.2, 141.5, 141.4, 140.3, 139.9, 135.2, 135.0, 134.64, 134.59, 134.5, 133.3, 129.9, 129.7, 129.5, 129.1, 128.5, 128.3, 128.1, 128.99, 127.96, 127.3, 127.0, 126.9, 126.8, 121.2, 120.9, 119.8, 117.4, 104.1 ppm. UV-Vis (DMF):  $\lambda_{\text{max}}$  ( $\epsilon$ ) 429 (98042), 523 (10377), 558 (2111.1), 601 (2886.4), 657 (5185.9) nm ( $\text{cm}^{-1} \text{M}^{-1}$ ). MS-ESI(+):  $m/z$  calculated for  $\text{C}_{51}\text{H}_{33}\text{ClN}_5\text{O}$  766.24  $[\text{M} + \text{H}]^+$  and 383.62  $[\text{M} + 2\text{H}]^{2+}$ ; found  $m/z$  766.33 and  $m/z$  383.72.

#### 2.4. Reactions of *p*-chlorophenoxyacetonitrile with the copper (II) and the zinc (II) complexes of 2-nitro-5,10,15,20-tetraphenylporphyrin

##### 2.4.1. Synthesis of compound 2-Cu

To a solution of *t*-BuOK (31.1 mg, 0.28 mmol) in 5 mL DMSO was added the metalloporphyrin **1-Cu** (20 mg, 0.028 mmol) and *p*-chlorophenoxyacetonitrile (9.9 mg, 0.059 mmol). The reaction mixture was stirred under nitrogen atmosphere at rt for 30 min. The mixture was then neutralized by the addition of a 3% HCl aq. solution (50 mL), washed with water, the organic layer extracted with  $\text{CH}_2\text{Cl}_2$  and the solvent was evaporated under reduced pressure. The crude mixture was purified by preparative thin-layer chromatography using toluene as the eluent. Compound **2-Cu** was obtained pure after crystallization from  $\text{CH}_2\text{Cl}_2$ /hexane.

2.4.1.1. [2-(Cyanomethyl)-3-nitro-5,10,15,20-tetraphenylporphyrinato]copper(II) **2-Cu**. Yield: 48% (10.1 mg, 13.2  $\mu\text{mol}$ ). UV-Vis (DMF):  $\lambda_{\text{max}}$  ( $\epsilon$ ) 423 (19576), 553 (3352), 598 (2661.6) nm ( $\text{cm}^{-1} \text{M}^{-1}$ ). MS-ESI(+):  $m/z$  calculated for  $\text{C}_{46}\text{H}_{29}\text{CuN}_6\text{O}_2$  760.16  $[\text{M} + \text{H}]^+$ ; found  $m/z$  760.32.

##### 2.4.2. Synthesis of compounds 5-Zna-c

To a solution of *t*-BuOK (31 mg, 0.2 mmol) in 5 mL DMSO was added the metalloporphyrin **1-Zn** (20 mg, 0.028 mmol) and *p*-chlorophenoxyacetonitrile (9.9 mg, 0.059 mmol). The reaction mixture was stirred under nitrogen atmosphere at rt. for 72 h. The mixture was then neutralized by the addition of a 3% HCl aq. solution (50 mL), washed with water, the organic layer extracted with  $\text{CH}_2\text{Cl}_2$  and the solvent was evaporated under reduced pressure. The crude mixture was purified by preparative thin layer chromatography using toluene as the eluent. The starting porphyrin was recovered in 32% and compounds **5-Zna-c** were obtained pure after crystallization from  $\text{CH}_2\text{Cl}_2$ /hexane.

2.4.2.1. [2-(4-chlorophenoxy)carbonyl]-5,10,15,20-tetraphenylporphyrinato]zinc(II), **5-Zna**. Yield: 22% (5.6 mg, 6.1  $\mu\text{mol}$ ).  $^1\text{H}$  NMR (300 MHz,  $\text{CDCl}_3$ ):  $\delta$  9.30 (1H, s, H- $\beta$ ), 8.96–8.88 (6H, m, H- $\beta$ ), 8.29–8.19 (8H, m, H-*o*-Ph), 7.85–7.72 (12H, m, H-*o,p*-Ph), 7.69–7.64 (3H, m, H-*o,p*-Ph), 7.34 (2H, d,  $J = 8.8$  Hz, H-PhCl), 7.00 (2H, d,  $J = 8.8$  Hz, H-PhCl) ppm.  $^{13}\text{C}$  NMR (125 MHz,  $\text{CDCl}_3$ ):  $\delta$  165.2 (CO), 151.3, 151.2, 151.03, 150.95, 150.0, 149.4, 146.1, 145.4, 142.8, 142.5, 142.3, 135.8, 135.4, 135.1, 134.54, 134.44, 133.4, 132.7, 132.61, 132.57, 132.4, 132.3, 130.9, 129.1, 127.90, 127.86, 127.8, 126.79, 126.75, 126.7, 124.5, 124.0, 123.0, 122.4, 121.7, 121.5, 121.4, 118.9 ppm. UV-Vis (DMF):  $\lambda_{\text{max}}$  ( $\epsilon$ ) 430 (190462), 566 (7538.7), 610 (5283.7) nm ( $\text{cm}^{-1} \text{M}^{-1}$ ). MS-

ESI(+):  $m/z$  calculated for  $\text{C}_{51}\text{H}_{32}\text{ClN}_4\text{O}_2\text{Zn}$  831.15  $[\text{M} + \text{H}]^+$ ; found  $m/z$  831.31.

2.4.2.2. [2-(4-chlorophenoxy)carbonyl]-3-nitro-5,10,15,20-tetraphenylporphyrinato]zinc(II), **5-Znb**. Yield: 9% (2.2 mg, 2.5  $\mu\text{mol}$ ).  $^1\text{H}$  NMR (300 MHz,  $\text{CDCl}_3$ ):  $\delta$  8.90–8.71 (5H, m, H- $\beta$ ), 8.75 (1H, d,  $J = 4.8$  Hz, H- $\beta$ ), 8.19–8.14 (8H, m, H-*o*-Ph), 7.80–7.61 (12H, m, H-*o,p*-Ph), 7.33 (2H, d,  $J = 8.6$  Hz, H-PhCl), 6.96 (2H, d,  $J = 8.6$  Hz, H-PhCl) ppm.  $^{13}\text{C}$  NMR (125 MHz,  $\text{CDCl}_3$ ):  $\delta$  153.0, 152.6, 152.5, 151.2, 141.9, 141.4, 139.8, 138.6, 135.4, 134.7, 134.4, 134.24, 134.20, 133.5, 132.8, 132.7, 131.4, 129.3, 128.8, 128.5, 127.9, 126.9, 126.63, 126.55, 122.8, 121.8, 121.1 ppm. UV-Vis (DMF):  $\lambda_{\text{max}}$  ( $\epsilon$ ) 437 (78831), 574 (4252.8), 624 (5127.7) nm ( $\text{cm}^{-1} \text{M}^{-1}$ ). MS-ESI(+):  $m/z$  calculated for  $\text{C}_{51}\text{H}_{31}\text{ClN}_5\text{O}_4\text{Zn}$  876.14  $[\text{M} + \text{H}]^+$ ; found  $m/z$  876.31.

2.4.2.3. [2-(4-chlorophenoxy)-3-formyl-5,10,15,20-tetraphenylporphyrinato]zinc(II), **5-Znc**. Yield: 8% (1.8 mg, 2.2  $\mu\text{mol}$ ).  $^1\text{H}$  NMR (300 MHz,  $\text{CDCl}_3$ ):  $\delta$  9.18 (1H, s, CHO), 8.95–8.85 (4H, m, H- $\beta$ ), 8.82 (1H, d,  $J = 4.7$  Hz, H- $\beta$ ), 8.69 (1H, d,  $J = 4.7$  Hz, H- $\beta$ ), 8.22–8.15 (6H, m, H-*o*-Ph), 7.85–7.69 (11H, m, H-*o,m,p*-Ph), 7.55–7.49 (1H, m, H-*p*-Ph), 7.40 (2H, t,  $J = 7.5$  Hz, H-*m*-Ph), 6.96 (2H, d,  $J = 9.0$  Hz, H-PhCl), 6.40 (2H, d,  $J = 9.0$  Hz, H-PhCl) ppm.  $^{13}\text{C}$  NMR (125 MHz,  $\text{CDCl}_3$ ):  $\delta$  187.3 (CHO), 158.0, 157.1, 151.8, 151.7, 151.4, 151.2, 151.1, 150.8, 144.8, 143.1, 142.2, 140.8, 137.3, 135.0, 134.5, 134.4, 133.4, 133.1, 133.0, 132.7, 132.5, 132.1, 129.9, 128.8, 128.6, 128.6, 127.8, 127.5, 126.8, 126.7, 126.5, 126.4, 126.2, 122.2, 121.5, 121.3, 120.5, 116.2 ppm. UV-Vis (DMF):  $\lambda_{\text{max}}$  ( $\epsilon$ ) 435 (97699), 571 (6039.9), 617 (4676.4) nm ( $\text{cm}^{-1} \text{M}^{-1}$ ). MS-ESI(+):  $m/z$  calculated for  $\text{C}_{51}\text{H}_{32}\text{ClN}_4\text{O}_2\text{Zn}$  831.15  $[\text{M} + \text{H}]^+$ ; found  $m/z$  831.32.

#### 2.5. Demetallation of the Cu(II) complex 2-Cu

Porphyrin **2-Cu** (15 mg, 0.02 mmol) was maintained under stirring in a 10% solution of  $\text{H}_2\text{SO}_4$  in  $\text{CHCl}_3$  (2 mL), at room temperature, for 15 min. Then, the mixture was carefully neutralized with an ice-cold aqueous solution of NaOH, the organic layer extracted with  $\text{CH}_2\text{Cl}_2$ , washed with water, dried with  $\text{Na}_2\text{SO}_4$  and the solvent was evaporated under reduced pressure. The crude mixture was purified by preparative thin layer-chromatography using toluene as the eluent. Compound **2** was obtained pure in almost quantitative yield after crystallization from  $\text{CH}_2\text{Cl}_2$ /hexane.

##### 2.5.1. 2-(Cyanomethyl)-3-nitro-5,10,15,20-tetraphenylporphyrin, **2**

Yield: 100% (13.8 mg, 19.7  $\mu\text{mol}$ ).  $^1\text{H}$  NMR (500 MHz,  $\text{CDCl}_3$ ):  $\delta$  8.96 (1H, d,  $J = 5.1$  Hz, H- $\beta$ ), 8.86–8.82 (2H, m, H- $\beta$ ), 8.67 (2H, s, H- $\beta$ ), 8.31–8.17 (8H, m, H-*o*-Ph), 7.91–7.69 (12H, m, H-*m,p*-Ph), 3.75 (2H, s,  $-\text{CH}_2\text{CN}$ ),  $-2.53$  (2H, s, *N*-H) ppm.  $^{13}\text{C}$  NMR (125 MHz,  $\text{CDCl}_3$ ):  $\delta$  157.5, 157.2, 153.4, 143.5, 141.2, 141.14, 141.08, 140.3, 139.6, 136.2, 135.4, 135.2, 134.9, 134.8, 134.7, 130.5, 130.0, 129.5, 128.9, 128.7, 128.4, 128.24, 128.18, 127.8, 127.1, 127.0, 122.2, 121.0, 120.7, 120.3, 116.8, 16.1 ( $-\text{CH}_2\text{CN}$ ) ppm. UV-Vis (DMF):  $\lambda_{\text{max}}$  ( $\epsilon$ ) 427 (124515), 529 (6669.2), 609 (1814.4), 672 (4107.3) nm ( $\text{cm}^{-1} \text{M}^{-1}$ ). MS-ESI(+):  $m/z$  calculated for  $\text{C}_{46}\text{H}_{31}\text{N}_6\text{O}_2$  699.25  $[\text{M} + \text{H}]^+$ ; found  $m/z$  699.40.

## 2.6. Mass spectrometry

Electrospray ionization mass spectra were acquired with a Micromass Q-ToF 2 (Micromass, Manchester, UK), operating in the positive ion mode, equipped with a Z-spray source, an electrospray probe and a syringe pump. Source and desolvation temperatures were 80 °C and 150 °C, respectively. Capillary voltage was 3000 V. The spectra were acquired at a nominal resolution of 9000 and at cone voltages of 30 V. Nebulisation and collision gases were N<sub>2</sub> and Ar, respectively. The porphyrin solutions of approximately 10<sup>-5</sup> M in methanol – 0.1% formic acid were introduced at a 10 μL.min<sup>-1</sup> flow rate. The MS/MS spectra presented were acquired by selecting the ion of interest with the quadrupole and using the hexapole as collision cell with energies from 35 to 55 eV.

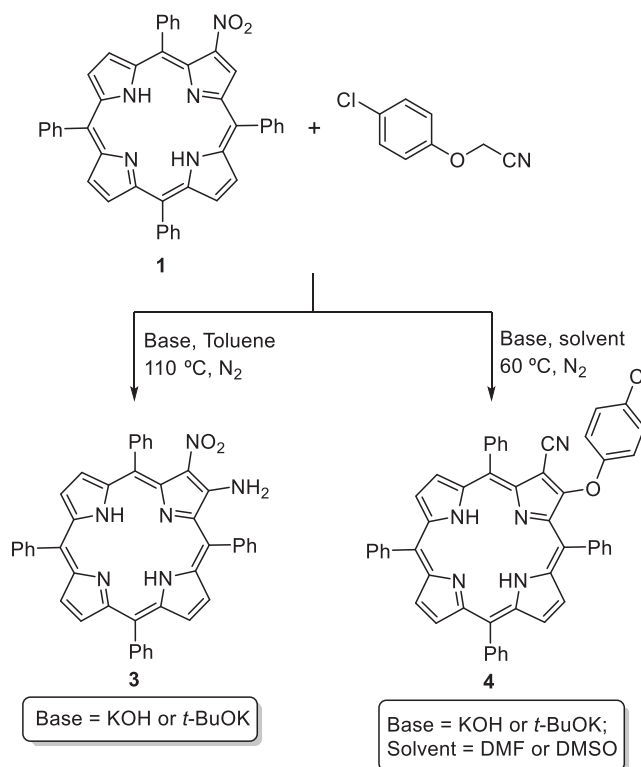
Ion Trap spectra were acquired using a Finnigan LXQ ion trap (Thermo Finnigan, San Jose, CA, USA) also in the positive ion mode. The source voltage was 4,99 kV, the capillary temperature and voltage were respectively 350 °C and 1 V, the pressure of the nitrogen sheath gas 30 psi. The same porphyrin solutions were introduced and the flow rate 8 μL min<sup>-1</sup>. MS<sup>n</sup> spectra were acquired by selecting and exciting chosen ions by standard isolation and excitation procedures.

## 3. Results and discussion

### 3.1. Synthesis

Considering that *p*-chlorophenoxyacetonitrile was reported as an efficient cyanomethylating agent of the Zn(II) complex of 2-nitro-5,10,15,20-tetraphenylporphyrin (Ostrowski & Raczko, 2005), we envisage that a similar approach could be extended to the corresponding free-base **β**-NO<sub>2</sub>TPP **1**. Under these conditions, it was expected to obtain the derivative with the cyanomethyl unit at the β-pyrrolic position adjacent to the nitro unit directly from the free-base, but a different outcome was found (Scheme 2 and Table S1).

The first experiments concerning the reaction of **β**-NO<sub>2</sub>TPP (**1**) with *p*-chlorophenoxyacetonitrile were performed in toluene, using KOH as base and under a nitrogen atmosphere (Scheme 2). Under these conditions, only at 110 °C it was possible to observe the consumption of the starting porphyrin **1** accompanied by the formation of a complex mixture of compounds (Table S1). After the work up, a careful purification of the crude mixture by preparative TLC using toluene as eluent, allowed us to isolate a compound which was characterized. The structure of this major product (obtained in 20% yield) was established as **3** based on its mass spectrum, which shows the [M + H]<sup>+</sup> ion at *m/z* 675.35, and NMR studies (see SI, Figs. S1–S7). The <sup>1</sup>H NMR spectrum reveals the signals due to the resonances of only six β-pyrrolic protons ranging from *ca.* δ 8.95 to δ 8.58 ppm. The protons of the *meso*-phenyl groups appear as a doublet at δ 8.35 ppm, three multiplets between *ca.* δ 8.2 and δ 7.7 ppm and one triplet at δ 7.49 ppm. The resonances of the protons from the amino group appear as a broad singlet at δ 6.80 ppm. The asymmetry of the macrocycle, induced by the presence of a nitro and an amino group at the β-pyrrolic positions of the same pyrrolic type unit, is confirmed by the presence of two singlets at high field, δ –2.33 and δ –2.57 ppm, due to the resonances of the inner *N*-H protons.



**Scheme 2** Products obtained in the reaction of **β**-NO<sub>2</sub>TPP with *p*-chlorophenoxyacetonitrile.

This dissimilarity in the resonances of the inner *N*-H protons is probably associated to an alteration in their tautomeric equilibrium, favouring one of the tautomers due to the presence of the two β-vicinal substituents (Vicente et al. 2012; Beletskaya et al. 2012; Thomas et al. 2020).

Richeter and co-workers (Richeter et al., 2007) reported a similar β,β'-disubstituted porphyrinic derivative by reaction of the Ni(II) and Cu(II) complexes of 2-nitro-5,10,15,20-tetrakis(4-*tert*-butylphenyl)porphyrin with the amination reagent 4-amino-4*H*-1,2,4-triazole. However, a literature survey shows that the preparation of porphyrinic derivatives analogues to compound **3** using the free-base **β**-NO<sub>2</sub>TPP is not reported.

The high level of decomposition observed and the moderate yield of compound **3** prompted us to test other bases (e.g. NaOH, Cs<sub>2</sub>CO<sub>3</sub> and *t*-BuOK; see Table S1) and lower temperatures; the best performance was observed in the presence of *t*-BuOK allowing to isolate compound **3** in slightly better yield, 28%. Under these conditions, no other compound was isolated in appreciable amounts. The reactions performed in the presence of the other bases and at lower temperatures were not effective, allowing mainly the recovery of the starting porphyrin **1**.

Under the same context to find better conditions for the reaction under study, a set of experiments were performed where toluene was replaced by DMF. Again, no products were detected at room temperature in the presence of any base after 24 h of reaction. However, when the reactions were performed in the presence of KOH or *t*-BuOK and heated at 60 °C, it was observed by TLC a total consumption of the starting material **1** after 30 min and 24 h of reaction, respectively. Once again,

the reaction leads to the formation of a complex mixture of compounds in small amounts. Nevertheless, after purification, we were able to isolate with both bases the same compound **4** (with  $m/z$  766.33). Again, the best performance was observed in the presence of *t*-BuOK (34% versus 13% in KOH). The synthesis of compound **4** was also achieved when the reaction was carried out in DMSO but in a lower yield (23%).

The structure of the new derivative was unambiguously established by spectroscopic data, namely NMR spectroscopic studies (see SI, Figs. S8–S11) and it is consistent with the structure of porphyrinic derivative **4**. The  $^1\text{H}$  NMR spectrum of derivative **4** presents the signals due to the resonance of six  $\beta$ -pyrrolic protons in the range of  $\delta$  8.92 to  $\delta$  8.71 ppm, thus confirming that a VNS reaction at the  $\beta$ -pyrrolic carbon adjacent to the nitro group had taken place. The signals due to the resonance of the protons from the *meso*-phenyl ring appear from *ca.*  $\delta$  8.25 to  $\delta$  7.50 ppm while the resonances of the protons from the *p*-chlorophenoxy unit appear as two doublets at  $\delta$  7.04 and  $\delta$  6.57 ppm. The singlet at  $\delta$  -2.80 ppm is attributed to the resonances of the inner *N*-H protons. The gas-phase fragmentation pattern observed for this derivative (*vide infra*) is also in accordance with the proposed structure.

The different outcomes conducting to the isolated compounds **3** and **4** (for mechanistic proposals see Section 3.3) are probably related with a better stabilization of the carbanion generated from *p*-chlorophenoxyacetonitrile in polar solvents, such as DMF or DMSO, favouring in this case the formation of the nitronate while in toluene the nucleophilic attack by the nitrogen atom from the acetonitrile group is preferential leading to the introduction of the amino group.

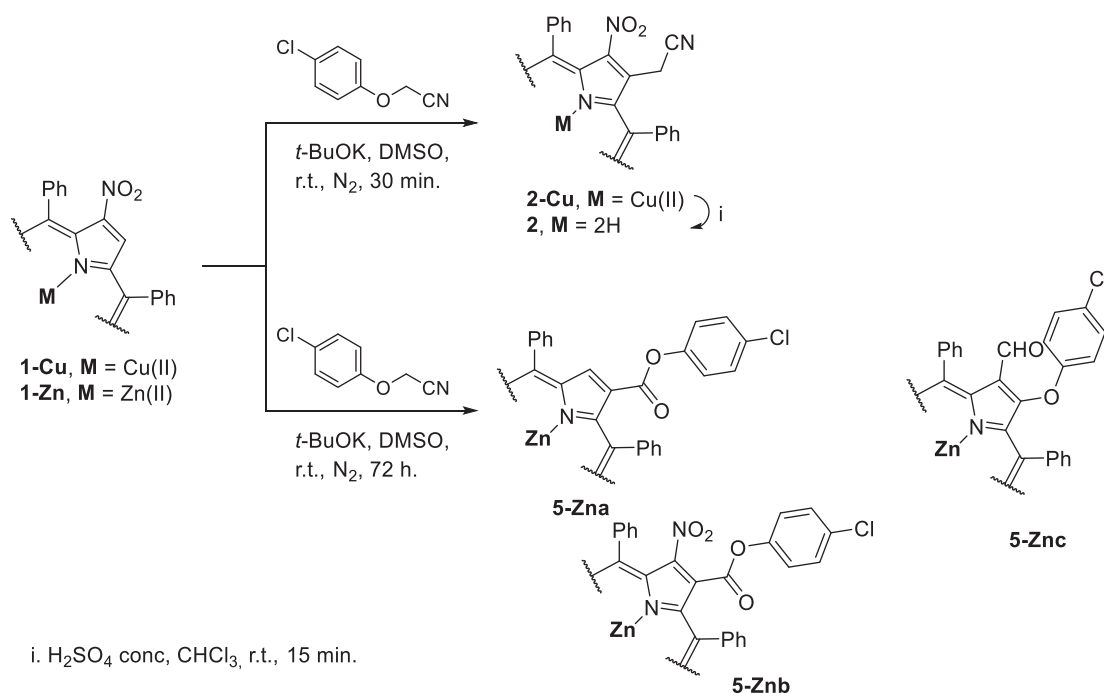
Based on the results obtained with the free-base 2-nitro-5,10,15,20-tetraphenylporphyrin **1**, and considering that the basic conditions are probably inducing an anionic character to the porphyrinic core not favourable to the desired nucleophilic reaction, we decided to protect the inner core of the

macrocycle with copper(II) and zinc(II) ions and to evaluate the reactivity of the corresponding complexes **1-Cu** and **1-Zn** in the presence of *p*-chlorophenoxyacetonitrile (Scheme 3).

When the reaction was performed with the Cu(II) complex **1-Cu**, in toluene, at 110 °C, in the presence of KOH or *t*-BuOK as bases, after 72 h, the formation of a complex mixture of compounds was observed. This fact prompted us to study the reaction under the conditions described by Ostrowski and co-workers (Ostrowski and Raczko, 2005) for the Zn(II) complex. So, the reaction of compound **1-Cu** with *p*-chlorophenoxyacetonitrile was performed in the presence of a large excess of *t*-BuOK in DMSO at r.t. and under a  $\text{N}_2$  atmosphere. After 30 min of reaction, the TLC control showed the total consumption of the starting porphyrin **1-Cu** and the formation of a new compound in an appreciable amount. After the work-up and purification by preparative TLC, the mass spectrum of the obtained compound is in accordance with the proposed structure **2-Cu**, presenting a peak at  $m/z$  760.32 corresponding to the  $[\text{M} + \text{H}]^+$  ion. Compound **2-Cu** isolated in 48% yield was treated with 10%  $\text{H}_2\text{SO}_4$  conc./ $\text{CHCl}_3$  in order to remove the paramagnetic metal ion; the expected free-base derivative **2** was obtained in almost quantitative yield.

The structure of compound **2** was supported by its mass spectrum, which shows the  $[\text{M} + \text{H}]^+$  ion at  $m/z$  699.40 and NMR data (Figs. S24–S27). The  $^1\text{H}$  NMR of compound **2** spectrum reveals the resonances of only six  $\beta$ -pyrrolic protons and a remarkable singlet at  $\delta$  3.75 ppm due to the resonance of the acetonitrile moiety at the  $\beta$ -pyrrolic position. The success of the decomplexation reaction is confirmed by the presence of a singlet at  $\delta$  -2.53 ppm assigned to the resonances of the inner core *N*-H protons.

When the reaction was carried out with the Zn(II) complex **1-Zn** under the same conditions three compounds in low yields (22%, 9% and 8%), were isolated and 32% of the starting por-



**Scheme 3** Reaction of the Cu(II) and Zn(II) complexes of 2-nitro-5,10,15,20-tetraphenylporphyrin with *p*-chlorophenoxyacetonitrile.

phyrin **1-Zn** was recovered. After purification, the structural analysis (Figs. S12–S23) allowed to conclude that the structures of the isolated compounds are in accordance with the structures of compounds **5-Zna-c** (see Scheme 3).

The  $^1\text{H}$  NMR spectrum of compound **5-Zna** (22%) shows a singlet at  $\delta$  9.30 ppm and a multiplet in the range  $\delta$  8.96–8.88 ppm due to the resonance of the seven  $\beta$ -pyrrolic protons. The protons resonance of the aryl group in the  $\beta$ -pyrrolic position appears as two doublets with a coupling constant of  $J$  8.8 Hz at  $\delta$  7.34 and  $\delta$  6.99 ppm. The presence of the ester unit is confirmed by the  $^{13}\text{C}$  NMR spectra that show a signal at  $\delta$  165.2 ppm.

The  $^1\text{H}$  NMR spectra of the minor compounds **5-Znb** (9%) and **5-Znc** (8%) show signals in the range from *ca.* 8.9 to *ca.* 8.7 ppm due to the resonance of only six  $\beta$ -pyrrolic protons, thus confirming the  $\beta,\beta'$ -disubstitution. In both cases, the presence of the *p*-substituted phenyl ring of the ether moiety is confirmed by the presence of two doublets in the range from  $\delta$  7.33 to  $\delta$  6.40 ppm. The  $^{13}\text{C}$  NMR spectrum of compound **5-Znc** shows a distinctive signal  $\delta$  187.3 ppm corresponding to the carbonyl carbon of the formyl unit. The mass spectra obtained for all derivatives are in accordance with the obtained NMR spectra.

Considering the important structural information given by gas-phase studies (Moura et al., 2016; Ramos et al., 2014; Ramos et al., 2015; Ramos et al., 2016), we decided to complement the knowledge about these unexpected compounds by performing MS/MS studies. It is important to refer that the absence in some of the proposed structures, of hydrogen atoms in one of the  $\beta$ -substituents, preclude an unequivocal structural identification of the obtained derivatives.

### 3.2. ESI-MS studies

As it was mentioned above and depending on the reaction conditions, the reaction of  $\beta\text{-NO}_2\text{TTP}$  with *p*-chlorophenoxyacetonitrile afforded, the unexpected compounds **3** and **4**. The protection of the inner core of  $\beta\text{-NO}_2\text{TTP}$  with copper ion gave the desired compound **2-Cu**, which, after demetallation, afforded the free-base **2**, while the protection with Zn(II) gave rise to compounds **5-Zna-c**. In order to simplify the discussion of the MS studies, the structural differences in what concerns the porphyrin core, the type of substituents, the monoisotopic mass and the mass of the more probable fragments are summarized in Table 1.

All the obtained compounds showed, in their mass spectra, the expected  $[\text{M} + \text{H}]^+$  ions (see Fig. S29). In the mass spectra of compounds **3** and **4**, the  $[\text{M} + 2\text{H}]^{2+}$  ions at  $m/z$  338.21 and 383.71 respectively, were also observed, probably due to the protonation in the inner core of the macrocycle and of basic sites present in the substituents.

The MS/MS spectra of the different derivatives were acquired by selecting the ion of interest with the quadrupole and using the hexapole as collision cell with energies from 35 to 55 eV. Based on the analysis of the obtained product-ion spectra, structures for some of the observed fragment ions were proposed.

In some of the proposals, reactions involving rearrangement/elimination triggered by the interaction between the *meso*-phenyl and the  $\beta$ -pyrrolic substituents were considered. Some of the proposed structures are in line with previous stud-

ies involving other porphyrin derivatives (Moura et al., 2016; Ramos et al., 2012; Ramos et al., 2014; Ramos et al., 2015; Ramos et al., 2016). The MS<sup>3</sup> spectra were obtained for the main fragment ions of the MS<sup>2</sup> spectra and the obtained results support the proposed structures.

To facilitate the analysis of the obtained results and considering the type of substituent present in the structure, the gas-phase behaviour of the derivatives will be discussed in two distinct groups. The derivatives **2**, **3** and **2-Cu** (without the chlorophenoxy substituent) in one group, and the derivatives **4**, **5-Zna**, **5-Znb** and **5-Znc** (with the chlorophenoxy substituent) in another group.

#### 3.2.1. Derivatives **2**, **3** and **2-Cu**

The free-bases **2** and **3** bear the same NO<sub>2</sub> unit in one of the  $\beta$  pyrrolic positions (R<sub>1</sub>) and differ in the R<sub>2</sub> substituent (CH<sub>2</sub>-CN *versus* NH<sub>2</sub>). Compound **2-Cu** is the Cu(II) complex of **2** so their  $\beta$ -substituents are the same (Table 1). The product ion spectra of the ions  $[\text{M} + \text{H}]^+$  were obtained in the same experimental conditions and are presented in Fig. 1; in these spectra, the precursor ions are indicated by asterisks (\*). The percentage of the base peak intensity of the main fragment ions observed, and the suggested losses are presented in Table 2.

The main product ions observed for these derivatives correspond to losses of one or two OH radicals, one water molecule or two in the case of compound **3**, loss of the substituent NO<sub>2</sub> (R<sub>1</sub>) and of both substituents R<sub>1</sub> and R<sub>2</sub> as radicals or combined with hydrogen.

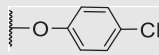
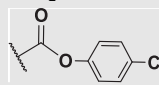
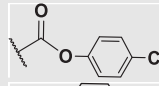
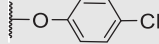
In the case of compound **3**, the most abundant product ion at  $m/z$  628.39 results from the loss of HNO<sub>2</sub> (HR<sub>1</sub>; or/and the combined loss of the radical NO<sub>2</sub> and a hydrogen atom) mediated by a five-membered intramolecular cyclization involving the adjacent *meso*-phenyl group (see in Scheme S1 the proposed structures for the formed fragments). The product ion at  $m/z$  613.38 (48.1%) can be justified by considering a similar intracyclization with the combined loss of the radicals NO<sub>2</sub> and NH<sub>2</sub>, probably as nitramide (NO<sub>2</sub>NH<sub>2</sub>). Six-membered intramolecular cyclization processes involving the nitrogen atom of the nitro group accompanied by the loss of one and two H<sub>2</sub>O molecules justify the product ions with  $m/z$  657.36 and 639.36, respectively.

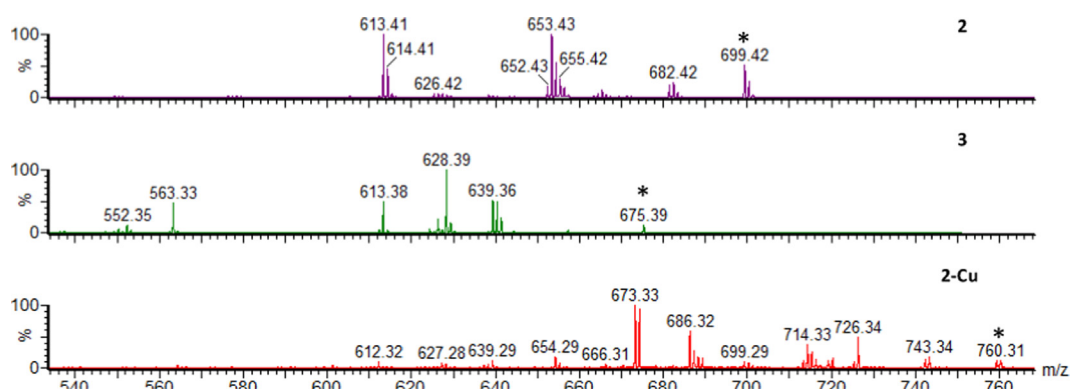
For compounds **2** and **2-Cu** (see Fig. 1 and Table 2), the structure of the fragment ions are, in general, similar although differing, as expected, by the presence of Cu(II) in the ions derived from **2-Cu**. These results suggest that the absence or the presence of Cu(II) in the inner core of the porphyrin did not affect the fragmentation pattern of these derivatives, although in relation with their abundance some differences can be found.

The structures proposed for the fragment ions observed in the case of compound **2** are presented in Scheme S2. For the free-base **2** the ion at  $m/z$  613.41 (100%) can also be justified by the loss of both substituents mediated by the five-membered cyclization; the second most abundant ion at  $m/z$  653.43 (84.9%) is just the result of the loss of the radical NO<sub>2</sub>. The formation of less abundant fragments due to losses of OH radicals and H<sub>2</sub>O were also facilitated by the intracyclization with the *meso*-phenyl groups as it is proposed in Scheme S2.

As can be observed in Table 2, for complex **2-Cu**, although the observed fragment similarity, the most abundant product

**Table 1** Formulae, monoisotopic masses and structure of studied compounds.

Compound	Monoisotopic masses (Da)	Formulae	Structure		fragment (Da)	R <sub>2</sub>	fragment (Da)
			M	R <sub>1</sub>			
2	698.24	C <sub>46</sub> H <sub>30</sub> N <sub>6</sub> O <sub>2</sub>	H	NO <sub>2</sub>	46	-CH <sub>2</sub> CN	40
3	674.24	C <sub>44</sub> H <sub>30</sub> N <sub>6</sub> O <sub>2</sub>	H	NO <sub>2</sub>	46	-NH <sub>2</sub>	16
4	765.23	C <sub>51</sub> H <sub>32</sub> N <sub>5</sub> ClO	H	CN	26		127
2-Cu	759.16	C <sub>46</sub> H <sub>28</sub> N <sub>6</sub> O <sub>2</sub> Cu	Cu	NO <sub>2</sub>	46	-CH <sub>2</sub> CN	40
5-Zna	830.14	C <sub>51</sub> H <sub>31</sub> N <sub>4</sub> ClO <sub>2</sub> Zn	Zn	H	1		155
5-Znb	875.13	C <sub>51</sub> H <sub>30</sub> N <sub>5</sub> ClO <sub>4</sub> Zn	Zn	NO <sub>2</sub>	46		155
5-Znc	830.14	C <sub>51</sub> H <sub>31</sub> N <sub>4</sub> ClO <sub>2</sub> Zn	Zn	CHO	29		127

**Fig. 1** Product ion spectra of the  $[M + H]^+$  ions of compounds **2**, **3** and **2-Cu**; \* – precursor ion.**Table 2** Fragment ions observed in the product ion spectra of compounds **2**, **3** and **2-Cu**; % BPI (percentage of base peak intensity).

Precursor ion	Compound					
	$[M + H]^+$ $m/z$ 699.42		$[M + H]^+$ $m/z$ 675.39		$[M + H]^+$ $m/z$ 760.31	
	2		3		2-Cu	
	fragments					
Loss	$m/z$	% BPI	$m/z$	% BPI	$m/z$	% BPI
-OH	682.42	23.2	–	–	743.34	18.7
-H <sub>2</sub> O	681.41	20.5	657.36	4.5	742.31	14.4
-2*OH	665.41	11.4	–	–	726.34	46.7
-2*H <sub>2</sub> O	–	–	639.36	51.1	–	–
-R <sub>1</sub>	653.43	84.9	–	–	714.33	42.5
-(R <sub>1</sub> + H)	–	–	628.39	100	–	–
-(R <sub>1</sub> + H + CN)	626.42	6.3	–	–	686.32	56.7
-(R <sub>1</sub> + R <sub>2</sub> )	613.41	100	613.38	48.1	674.33	95.5
-(R <sub>1</sub> + R <sub>2</sub> + H)	–	–	–	–	673.33	100



ions are the ions with  $m/z$  673.33 (100%) and 674.33 (95.5%) and they can be justified by a five-membered intramolecular cyclization accompanied by the combined loss of both substituents plus a hydrogen atom and of just both substituents.

It is interesting to observe that independently from the substituents present in the structures, most of the formed fragments result on a cyclization process, the structures being, in most of the cases, stabilized by resonance. This can be justified with the occurrence of charge delocalization and consequent increase in the fragment stability. The formation of similar fragments by cyclization was previously described by other authors (Domingues et al., 2001; Izquierdo et al., 2007; Silva et al., 2005). Interestingly, similar intramolecular cyclization involving  $\beta$ -pyrrolic position and adjacent *meso*-phenyl groups were also reported in solution (Faustino et al., 1995, 2005; Saegusa et al., 2015; Vale et al., 2007).

From the analysis of the obtained fragments, it was possible to conclude that the fragmentation process depends on the site of protonation and probably for that there is an equilibrium between those structures; this can be easily rationalized by considering the multiple basic sites present in the different compounds.

### 3.2.2. Derivatives 4 and 5-Zna-c

In the second series of compounds the presence of the *p*-chlorophenoxy substituent is common to all the derivatives. This unit appears directly linked to the  $\beta$ -pyrrolic position in compound 4 (with  $R_1 = \text{CN}$ ) and in compound 5-Znc ( $R_1 = \text{CHO}$ ). In the other derivatives, it appears as a *p*-chlorophenoxy-carbonyl unit, and for compound 5-Zna it is the only substituent. For compound 5-Znb the other  $\beta$ -pyrrolic position is substituted by the nitro group.

The product ion spectra of the  $[\text{M} + \text{H}]^+$  ions of the derivatives under analysis is presented in Fig. 2 and again each precursor ion is assigned with an asterisk (\*). The percentage of the main fragment ions observed in those spectra and the suggested losses are summarized in Table 3.

The main fragments observed for these derivatives result from the loss of the *p*-chlorophenoxy substituent or from the combined loss of both substituents  $R_1$  and  $R_2$ .

For derivative 4, the most abundant product ion appears at  $m/z$  639.37 (100%) due to the loss of the *p*-chlorophenoxy radical

( $R_2\bullet$ ) and the second most abundant at  $m/z$  562.34 (31.6%) is due to the combined loss of  $R_2^\bullet$  and  $\text{Ph}^\bullet$  substituents (see proposed structures in Scheme S3). So, for this compound the main fragmentations result from homolytic cleavages of substituents and does not involve cyclization process. The loss of the  $R_1$  substituent (CN) is not observed, however a less abundant fragment ion at  $m/z$  623.34 (10.8%) resulting from the combined loss mediated by cyclization process of the *p*-chlorophenoxy and of the nitrogen atom of the  $R_1$  substituent is observed.

Also for compound 4, from the analysis of the  $\text{MS}^3$  spectrum of the  $[\text{M} + \text{H}]^+ \rightarrow m/z$  639.42  $\rightarrow$  products (Fig. S30) it was possible to observe an ion at  $m/z$  638.5, due to the elimination of a hydrogen atom, and another one at  $m/z$  623.42 due to the loss of  $\text{NH}_2$  as a radical and at  $m/z$  612.42 due to the loss of HCN. However, the most intense peak appears at  $m/z$  562.42 due to the homolytic cleavage of a  $\text{Ph}^\bullet$  substituent.

When comparing the behaviour of the derivatives 5-Zna-c it was possible to observe that the ion with  $m/z$  676.3 is common to all of them, being the most abundant one for compounds 5-Znb and 5-Znc (Scheme S4). The homolytic cleavage of the *p*-chlorophenoxy-carbonyl unit can easily justify the formation of this fragment from 5-Zna. However, for the other derivatives, probably an intramolecular reaction occurs between both substituents  $R_1$  and  $R_2$  before their elimination as radicals. Again, an equilibrium between structures protonated at different basic sites can be rationalized due to their presence in the different compounds.

Along with this fragment ion, other fragments resulting from cyclization processes with the phenyl groups of *meso* positions are observed as it is shown in Scheme 4. In fact, for derivative 4, the most abundant product ion ( $m/z$  703.32) is a result of an intracyclization process with the carbonyl group of the ester group accompanied by the loss of *p*-chlorophenol. In solution, an analogous intracyclization was reported during attempts to demetallate the Cu(II) complex of 2-formyl-5,10,15,20-tetraphenylporphyrin (Henrick et al., 1980).

Similar intracyclizations can justify the less abundant fragments ions that appear at  $m/z$  704.31 and  $m/z$  686.31 respectively for derivatives 5-Znb and 5-Znc.

The same samples were also analysed in the Ion Trap instrument, in order to obtain the  $\text{MS}^3$  spectra of the most abundant ions and support the structure present in the sub-

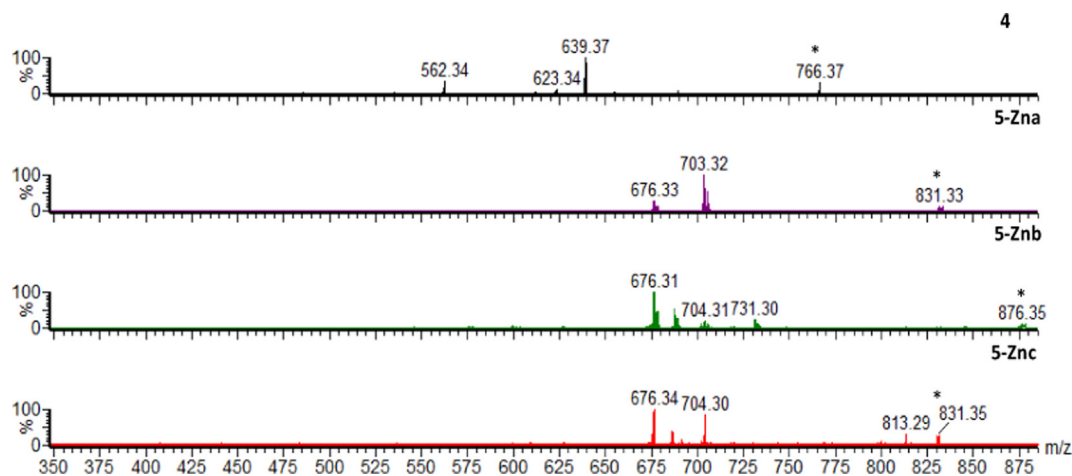
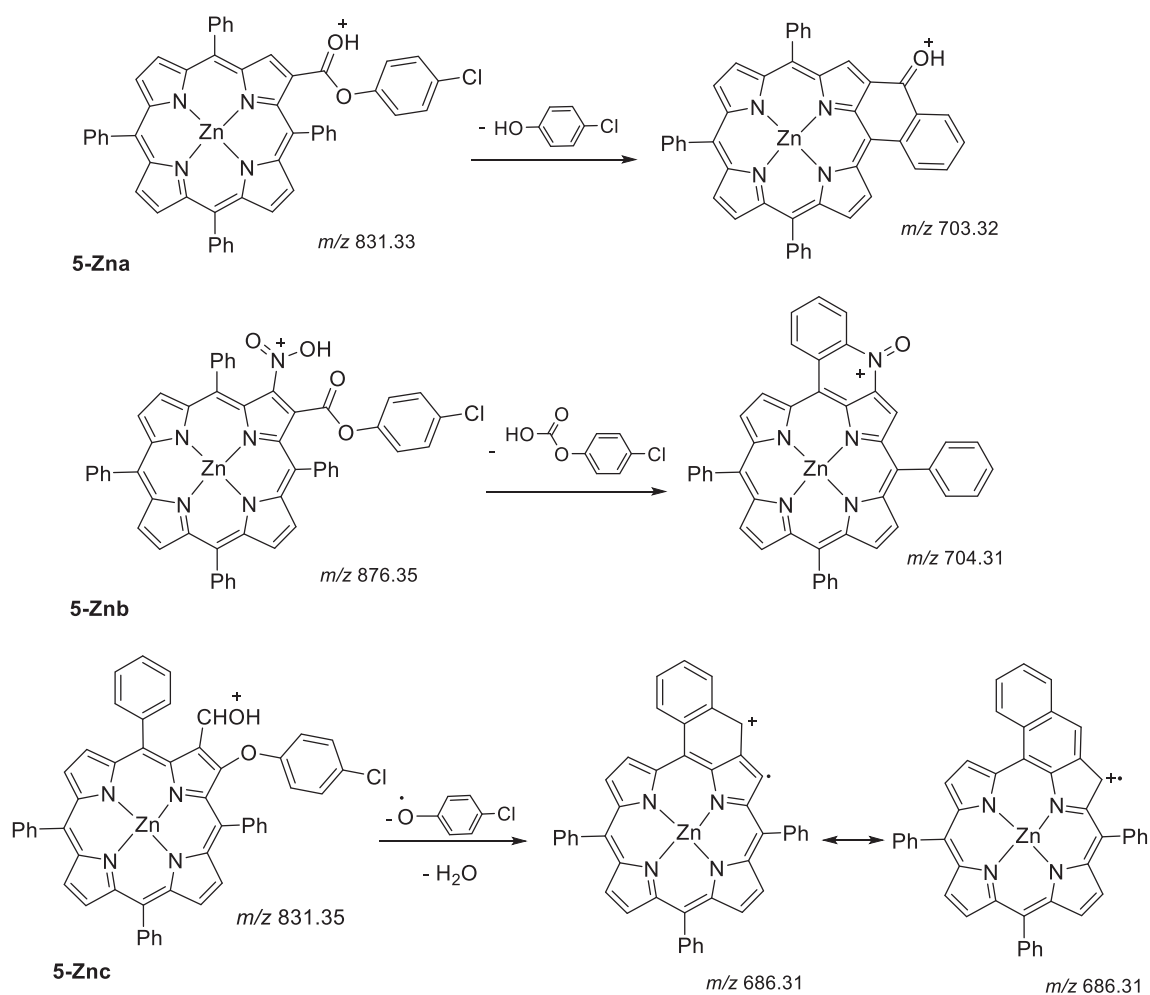


Fig. 2 Product ion spectra of the  $[\text{M} + \text{H}]^+$  ions of compounds 4, 5-Zna, 5-Znb and 5-Znc; \* – precursor ion.

**Table 3** Fragment ions observed in the product ion spectra of compounds **4** and **5-Zna-c**.

Precursor ion [M + H] <sup>+</sup>	Compound							
	4		5-Zna		5-Znb		5-Znc	
	<i>m/z</i> 766.37		<i>m/z</i> 766.37		<i>m/z</i> 766.37		<i>m/z</i> 766.37	
	Fragments							
loss	<i>m/z</i>	% BPI	<i>m/z</i>	% BPI	<i>m/z</i>	% BPI	<i>m/z</i>	% BPI
-H <sub>2</sub> O							813.29	26.3
-(OC <sub>6</sub> H <sub>4</sub> Cl + H)			703.32	100				
-(OC <sub>6</sub> H <sub>4</sub> Cl + H <sub>2</sub> O)					731.30	24.1		
-R <sub>2</sub>	639.37	100	676.33	28.4			704.30	33.5
-(R <sub>2</sub> + OH)					704.31	18.8		
-(R <sub>2</sub> + H <sub>2</sub> O)							686.30	17.4
-(R <sub>2</sub> + 2 OH)					687.31	51.7		
-[(R <sub>1</sub> + R <sub>2</sub> ) - H]					676.31	100	676.34	100
-(NH <sub>2</sub> + R <sub>2</sub> )	623.34	10.8						
-(R <sub>2</sub> + Ph)	562.34	31.6						

% BPI - (percentage of base peak intensity).

**Scheme 4** Proposed structures for fragment ions of protonated compounds **5-Zna-c**.

stituents, and consequently the proposed structures for the new derivatives. By analysing the obtained MS<sup>3</sup> spectrum of the

most abundant ions it was possible to support the proposed structures of all the derivatives.

For derivatives **4** and **5-Znc**, the MS<sup>3</sup> spectra of [M + H]<sup>+</sup> → *m/z* 639.42 → products (for **4**) and the spectrum [M + H]<sup>+</sup> → *m/z* 704.35 → products (for **5-Znc**) were obtained; also the loss in the first case corresponding to an HCN and in the second one of a CO loss led us to confirm the proposed structures (Figs. S30 and S31).

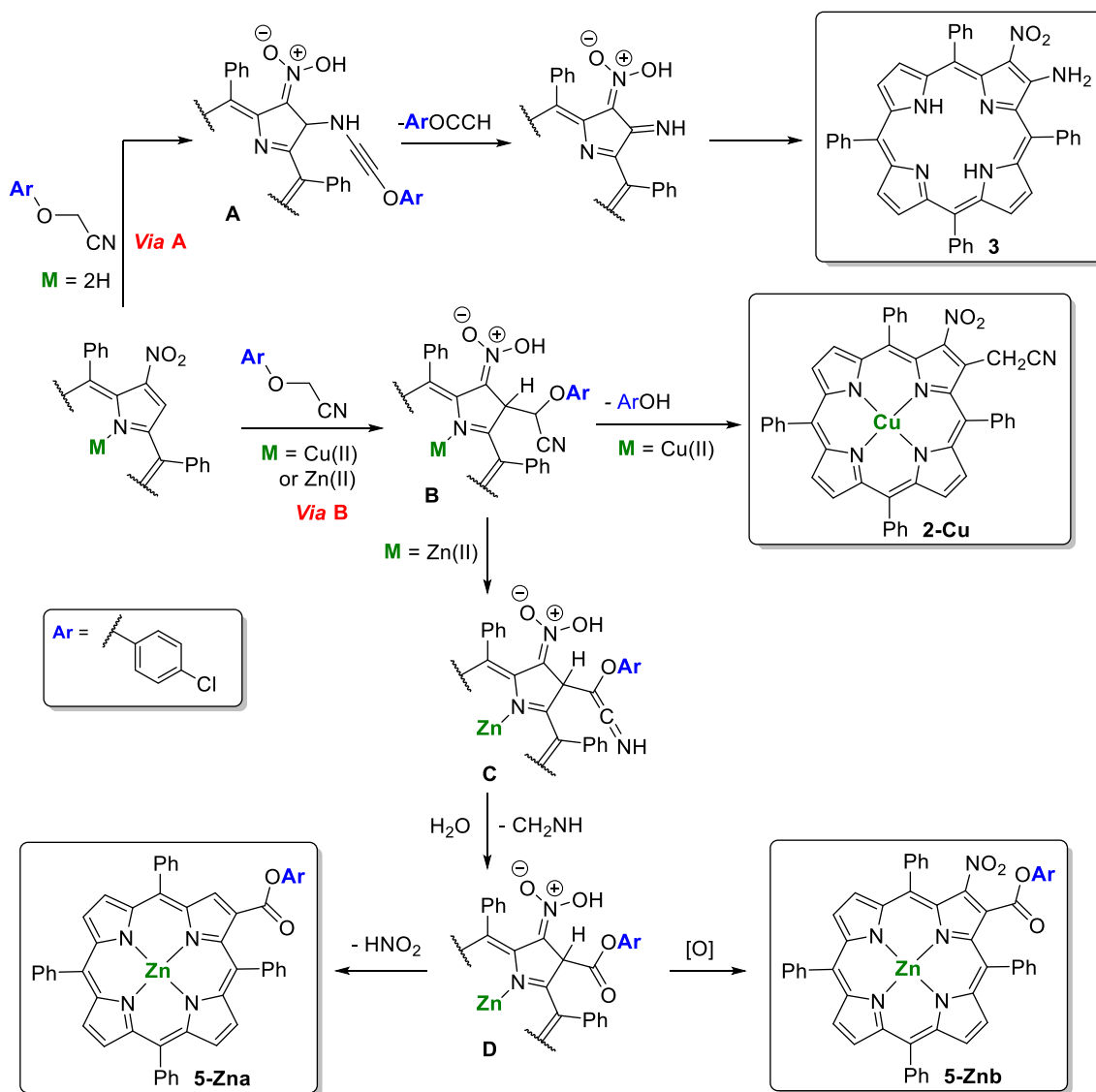
### 3.3. Mechanistic considerations

A probable pathway leading to the formation of the compounds obtained from the reaction of the *p*-chlorophenoxyacetonitrile with the β-nitroTPP derivatives are outlined Schemes 5 and 6. Considering the structure of the compounds obtained, only the copper(II) complex of β-nitroTPP (**1-Cu**, M = Cu) follows the expected pathway: the initial attack of the carbanion at the β-pyrrolic position adjacent to the nitro group leads to intermediate **B** (Scheme 5, Via B) which after the loss of *p*-chlorophenol gives rise to derivative **2-Cu**. In the presence of the Zn(II) complex of β-nitroTPP (**1-Zn**, M = Zn) the intermediate **B** after a pro-

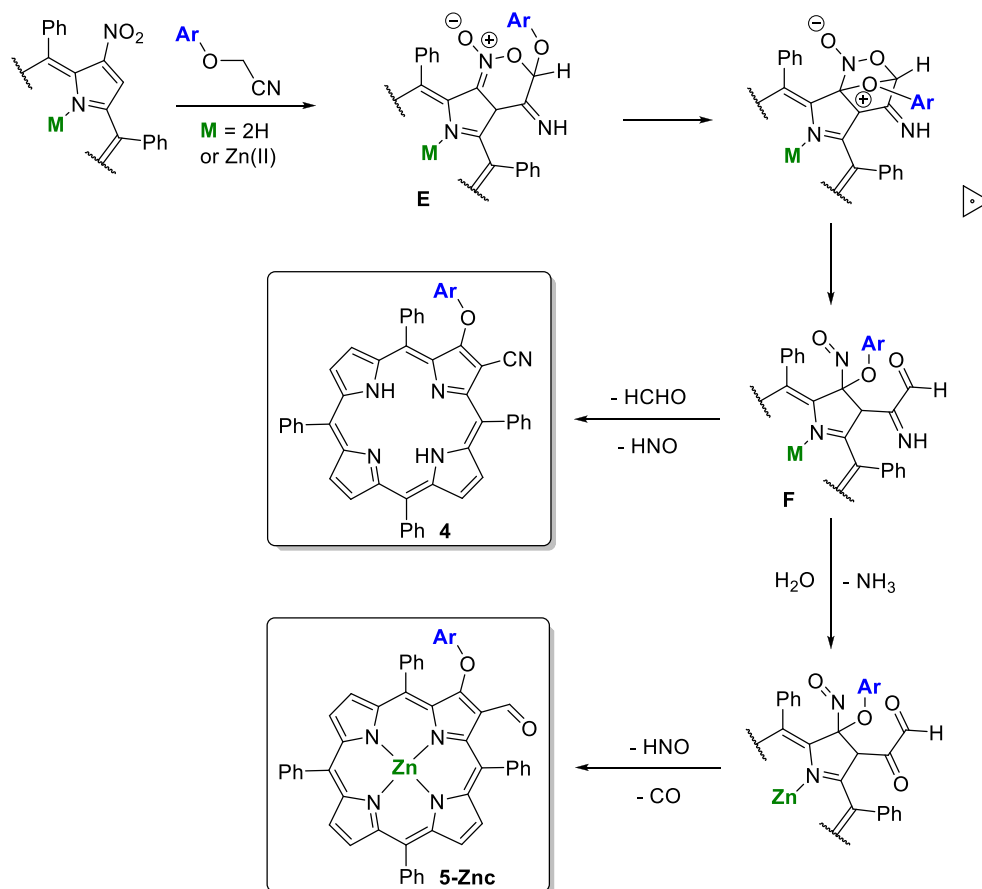
toprotic tautomerization pathway leads to intermediated **C** that can suffer hydrolysis and elimination of CH<sub>2</sub> = NH (or CH<sub>2</sub>O, NH<sub>3</sub>) giving rise to species **D**. The loss of HNO<sub>2</sub> from this intermediate affords compound **5-Zna** while its oxidation can explain the formation of **5-Znb**.

The formation of derivative **3** (Scheme 5, Via A) requires the attack of the nitrogen from the *p*-chlorophenoxyacetonitrile at the β-pyrrolic position adjacent to the nitro group (Ritter type approach). The elimination of ArOCCH from the intermediate **A** followed by a prototropic tautomerization can explain the formation of this product bearing both functionalities, the nitro and the amino substituents, at adjacent β-pyrrolic positions.

The formation of compounds **4** and **5-Znc** (Scheme 6) can start with the formation of the six-membered nitronate **E** (Tabolin et al., 2017). Then, the intramolecular attack of the phenoxy oxygen at the *ipso* position generates **F** that can lose HCHO and HNO affording compound **4**. The hydrolysis of the imine accompanied by loss of HNO and CO can explain the formation of derivative **5-Znc**.



Scheme 5 Mechanistic pathway proposed for the synthesis of compounds **3**, **2-Cu** and **5-Zna,b**.



**Scheme 6** Mechanistic pathway proposed for the synthesis of compounds **4** and **5-Znc**.

As it was expected all the compounds isolated resulted from reactions occurring at the pyrrole unit substituted with the nitro substituent, although the expected cyanomethyl derivative was obtained only when the porphyrin inner core was protected with the copper(II) metal ion. The different outcomes imposed by the coordinated metal ions can be rationalized having into account their important inductive effect on the  $\pi$ -electron system able to influence the chemical reactivity (Vicente et al., 2012; Jaquinod et al. 2000). For instance, it is known that closed-shell configuration metals like Zn(II) induce a high negative charge onto the porphyrin periphery, favoring the electrophilic attack. On the other hand, metals like Cu(II) capable of  $\pi$ -back-bonding decrease the electron density on the macrocycle. Considering this, it is expected that the electron-withdrawing character of the nitro is favored by the presence of Cu(II) ion due to its ability to reduce the electron density of macrocycle and consequently to favor the nucleophilic attack at the adjacent position to the nitro group and the further loss of *p*-chlorophenol. On the other hand, in the case of the Zn(II) complex with the increase of the electron density on the macrocycle the situation is not advantageous to the nucleophilic attack and to the elimination of *p*-chlorophenol allowing parallel prototropic tautomerizations to occur and being responsible for the formation of derivatives **5-Zna,b**. It is also possible that the better fitting of the Cu(II) ion into the porphyrin inner core, when compared with the Zn(II) ion, can minimize the parallel prototropic tautomerizations leading to the non-expected derivatives.

Considering the free-base, the expected nucleophilic attack by *p*-chlorophenoxyacetonitrile carbanion is probably being affected by some anionic features of the macrocycle due to the removal of the inner core protons under basic conditions, allowing parallel reactions. In toluene the formation/stabilization of the carbanion is less favorable, inducing in that way the attack of the nitrogen atom from the nitrile and affording compound **3**, while in the polar solvents (DMF or DMSO) a better stabilization conducted to the formation of the six-membered nitronate **E** giving rise to product **4**. Interestingly, this same intermediate can justify the formation of **5-Znc** which is in line with the importance of the electron density induced into the macrocycle core.

It is important to highlight that these parallel reactions were not detected in studies involving *p*-chlorophenoxyacetonitrile and simpler systems like nitroindazoles, where the expected cyanomethyl derivatives were obtained (Eddahmi et al., 2019b).

#### 4. Conclusions

In summary, the study involving the reaction of 2-nitro-5,10,15,20-tetraphenylporphyrin with *p*-chlorophenoxyacetonitrile showed that the outcome of the reaction can be modulated by the absence or presence of the coordinated metal ion, and solvent.

We found that *p*-chlorophenoxyacetonitrile which is recognized as an efficient cyanomethylating agent for the Zn(II)

complex of  $\beta$ -NO<sub>2</sub>TPP, can lead, depending on the experimental conditions, to an interesting range of  $\beta,\beta'$  substituted derivatives. Contrary to what was previously reported in the literature only when the inner core of the porphyrin was coordinated with copper(II) it was possible to isolate derivative **2-Cu** with the required cyanomethyl functionality. The porphyrins with other functionalities at adjacent  $\beta$ -pyrrolic positions like nitro/amino and CN/*p*-chlorophenoxy were isolated when the free-base was used, and their formation was dependent on the solvent used. The Zn(II) complex afforded mono- and di-substituted porphyrinoids with an ester functionality and a derivative with a formyl adjacent to the *p*-chlorophenoxy substituent. Further studies on the synthetic approaches here described can open new ways to obtain compounds with improved features to be used in several fields, from medicine to materials and sensors, by taking profit of the functional groups presented in the molecules for further modifications or immobilization in solid supports. A mechanistic rationalization for the formation of these compounds suggests that in general the attack of the carbanion occurs at the  $\alpha$  position of the nitro group but depending on the reaction conditions the loss of the *p*-chlorophenol seems not to be always favourable. Interestingly, the attack of nitrogen from the nitrile unit could explain the formation of derivative **3**. The fragmentation patterns obtained from the MS studies of the new derivatives show that, in general, intramolecular cyclizations with the formation of five and six-membered rings are responsible for the formation of the main fragment ions.

#### Declaration of Competing Interest

The authors declare that they have no known competing financial interests or personal relationships that could have appeared to influence the work reported in this paper.

#### Acknowledgments

Thanks are due to the University of Aveiro and FCT/MCT for the financial support for the QOPNA research Unit (FCT UID/QUI/00062/2019), the LAQV-REQUIMTE (UIDB/50006/2020), through national funds and, where applicable, co-financed by the FEDER, within the PT2020 Partnership Agreement, and to the Portuguese NMR Network. The authors also thank to the Sultan Moulay Slimane University and the Transnational cooperation programs, FCT-CNRST (Morocco), for financial assistance (2019-2020). The research contracts of N.M.M. Moura (REF.-048-88-ARH/2018) and C.I.V. Ramos (REF.-047-88-ARH/2018) are funded by national funds (OE), through FCT - Fundação para a Ciência e a Tecnologia, I.P., in the scope of the framework contract foreseen in the numbers 4, 5 and 6 of the article 23, of the Law Decree 57/2016, of August 29, changed by Law 57/2017, of July 19.

#### Appendix A. Supplementary material

Supplementary data to this article can be found online at <https://doi.org/10.1016/j.arabj.2020.04.022>.

#### References

Alonso, C.M.A., Neves, M.G.P.M.S., Tomé, A.C., Silva, A.M.S., Cavaleiro, J.A.S., 2005. Reaction of (2-amino-5,10,15,20-

- tetraphenylporphyrinato)nickel(II) with quinones. *Tetrahedron* 61 (50), 11866–11872.
- Amiri, O., Moura, N.M.M., Faustino, M.A.F., Cavaleiro, J.A.S., Rakib, E., Neves, M.G.P.M.S., 2019. Synthetic access to new porphyrinoids from 2-nitro-5,10,15,20-tetraphenylporphyrin and an arylacetoneitrile. *Monatsh. Chem.* 150 (1), 67–75.
- Armarego, W.L.F., Chai, C., 2013. *Purification of Laboratory Chemicals*. Butterworth-Heinemann, Oxford, UK.
- Auwärter, W., Ćejić, D., Klappenberger, F., Barth, J.V., 2015. Porphyrins at interfaces. *Nat. Chem.* 7, 105.
- Baldwin, J.E., Crossley, M.J., De Bernardis, J., 1982. Efficient peripheral functionalization of porphyrins. *Tetrahedron* 38 (5), 685–692.
- Beletskaya, P., Tyurin, V.S., Uglov, A., Stern, C., Guillard, R., 2012. The handbook of Porphyrin Science. In: Kadish, K.M., Smith, K. M., Guillard, R. (Eds.), World Scientific Publishers: Singapore, Vol. 23, pp. 81–279. (Chapter 108).
- Calvete, M.J.F., Pinto, S.M.A., Pereira, M.M., Geraldes, C.F.G.C., 2017. Metal coordinated pyrrole-based macrocycles as contrast agents for magnetic resonance imaging technologies: synthesis and applications. *Coord. Chem. Rev.* 333 (Supplement C), 82–107.
- Cen, T.Y., Wang, S.P., Zhang, Z.B., Wu, J., Li, S.J., 2018. Flexible porphyrin cages and nanorings. *J. Porphyrins Phthalocyanines* 22 (9–10), 726–738.
- Cerqueira, A., Moura, N.M.M., Serra, V.V., Faustino, M.A.F., Tomé, A.C., Cavaleiro, J.A.S., Neves, M.G.P.M.S., 2017.  $\beta$ -formyl- and  $\beta$ -vinylporphyrins: magic building blocks for novel porphyrin derivatives. *Molecules* 22 (8), 1269.
- Chang, K.P., Kolli, B.K., New Light, G., 2016. New “light” for one-world approach toward safe and effective control of animal diseases and insect vectors from leishmaniac perspectives. *Parasites Vectors* 9, 13.
- Costentin, C., Robert, M., Savéant, J.-M., 2015. Current issues in molecular catalysis illustrated by iron porphyrins as catalysts of the CO<sub>2</sub>-to-CO electrochemical conversion. *Acc. Chem. Res.* 48 (12), 2996–3006.
- Di Carlo, G., Biroli, A.O., Pizzotti, M., Tessore, F., 2019. Efficient sunlight harvesting by A(4) beta-pyrrolic substituted Zn-II porphyrins: a mini-review. *Front. Chem.* 7, 22.
- Di Carlo, G., Biroli, A.O., Tessore, F., Caramori, S., Pizzotti, M., 2018. beta-Substituted Zn-II porphyrins as dyes for DSSC: a possible approach to photovoltaic windows. *Coord. Chem. Rev.* 358, 153–177.
- Ding, Y., Zhu, W.-H., Xie, Y., 2017. Development of ion chemosensors based on porphyrin analogues. *Chem. Rev.* 117 (4), 2203–2256.
- Domingues, M.R.M., Graça, O.S., Marques, M., Domingues, P., Neves, M.G.P.M.S., Cavaleiro, J.A.S., Ferrer-Correia, A.J., Gross, M.L., 2001. Differentiation of positional isomers of nitro meso-tetraphenylporphyrins by tandem mass spectrometry. *J. Am. Soc. Mass Spectrom.* 12 (4), 381–384.
- Eddahmi, M., Moura, N.M.M., Bouissane, L., Faustino, M.A.F., Cavaleiro, J.A.S., Paz, F.A.A., Mendes, R., Figueiredo, J., Carvalhoe, J., Cruz, C., Neves, M.G.P.M.S., Rakib, E.M., 2019a. Synthesis and biological evaluation of new functionalized nitroindazolylacetoneitrile derivatives. *ChemistrySelect* 4, 14335–14342.
- Eddahmi, M., Moura, N.M.M., Bouissane, L., Gamouh, A., Faustino, M.A.F., Cavaleiro, J.A.S., Paz, F.A.A., Mendes, R., Lodeiro, C., Santos, S.M., Neves, M.G.P.M.S., Rakib, E.M., 2019b. New nitroindazolylacetoneitriles: efficient synthetic access via vicarious nucleophilic substitution and tautomeric switching mediated by anions. *New J. Chem.* 43, 14355–14367.
- El Abiad, C., Radi, S., Faustino, M.A.F., Neves, M., Moura, N.M.M., 2019. Supramolecular hybrid material based on engineering porphyrin hosts for an efficient elimination of lead(II) from aquatic medium. *Molecules* 24 (4), 21.
- Faustino, M.A.F., Neves, M.G.P.M.S., Tomé, A.C., Silva, A.M.S., Cavaleiro, J.A.S., 2005b. Diels-Alder reactions of beta-vinyl-meso-tetraphenylporphyrin with quinones. *ARKIVOC* (ix), 332–343.

- Hamblin, M.R., Abrahamse, H., 2018. Inorganic salts and antimicrobial photodynamic therapy: mechanistic conundrums? *Molecules* 23 (12), 18.
- Imran, M., Ramzan, M., Qureshi, A.K., Khan, M.A., Tariq, M., 2018. Emerging applications of porphyrins and metalloporphyrins in biomedicine and diagnostic magnetic resonance imaging. *Biosensors* 8 (4), 17.
- Ishkov, Y.V., 1999. Synthesis and properties of  $\beta$ -modified mesotetra (aryl, heteryl)porphyrins. *J. Appl. Spectrosc.* 66 (4), 561–565.
- Izquierdo, R.A., Barros, C.M., Santana-Marques, M.G., Ferrer-Correia, A.J., Silva, E.M.P., Giuntini, F., Pais, A.C., 2007. Characterization of isomeric cationic porphyrins with  $\beta$ -pyrrolic substituents by electrospray mass spectrometry: the singular behavior of a potential virus photoinactivator. *J. Am. Soc. Mass Spectrom.* 18 (2), 218–225.
- Cavaleiro, J.A.S., Tomé, A.C., Neves, M.G.P.M.S., 2010. Handbook of porphyrin science. In: Smith, K., Kadish, K.M., Guillard, K.M.R. (Eds.). *Meso-tetraarylporphyrin Derivatives: New Synthetic Methodologies*, Vol. 2. Singapore: World Scientific Publishing Company Co. pp. 193–294.
- Chaudri, N., Grover, N., Sankar, M., 2017. Versatile synthetic route for  $\beta$ -functionalized chlorins and porphyrins by varying the size of Michael donors: syntheses, photophysical, and electrochemical redox properties. *Inorg. Chem.* 56, 11532–11545.
- Faustino, M.A.F., Neves, M.G.P.M.S., Vicente, M.G.H., Silva, A.M.S., Cavaleiro, J.A.S., 1995. New naphthochlorins from the intramolecular cyclization of  $\beta$ -vinyl-meso-tetraarylporphyrins. *Tetrahedron Lett.* 36 (33), 5977–5978.
- Gros, C.P., Jaquinod, L., Khoury, R.G., Olmstead, M.M., Smith, K.M., 1997. Approaches to  $\beta$ -fused porphyrinoporphyryns: pyrrolo- and dipyrromethaneporphyrins. *J. Porphyrins Phthalocyanines* 1, 201–212.
- Higashino, T., Imahori, H., 2015. Porphyrins as excellent dyes for dye-sensitized solar cells: recent developments and insights. *Dalton Trans.* 44, 448–463.
- Jaquinod, L., 2000. Functionalization of 5,10,15,20-tetra-substituted porphyrins. In: Kadish, K.M.S.K.M., Guillard, R. (Eds.). *The Porphyrin Handbook*, Vol. 1. Academic Press, San Diego, pp. 212–222.
- Jaquinod, L., Gros, C., Olmstead, M.M., Antolovich, M., Smith, K.M., 1996. First syntheses of fused pyrroloporphyrins. *Chem. Commun.* 12, 1475–1476.
- Jaquinod, L., Gros, C.P., Khoury, R.G., Olmstead, M.M., Smith, K.M., 1997. A convenient synthesis of functionalized tetraphenylchlorins. *Chem. Commun.*, 2581–2582.
- Jenni, S., Sour, A., 2019. Molecular theranostic agents for photodynamic therapy (PDT) and magnetic resonance imaging (MRI). *Inorganics* 7 (1), 13.
- Jurow, M., Schuckman, A.E., Bateas, J.D., Drain, C.M., 2010. Porphyrins as molecular electronic components of functional devices. *Coord. Chem. Rev.* 254 (19), 2297–2310.
- Kadish, K.M., Smith, K.M., Guillard, R., 2010. In: *Handbook of Porphyrin Science*, Vol. 1–12. World Scientific Publishing Company Co., Singapore.
- Kc, C.B., D'Souza, F., 2016. Design and photochemical study of supramolecular donor-acceptor systems assembled via metal-ligand axial coordination. *Coord. Chem. Rev.* 322, 104–141.
- Keane, P.M., Kelly, J.M., 2018. Transient absorption and time-resolved vibrational studies of photophysical and photochemical processes in DNA-intercalating polypyridyl metal complexes or cationic porphyrins. *Coord. Chem. Rev.* 364, 137–154.
- Kundu, S., Patra, A., 2017. Nanoscale strategies for light harvesting. *Chem. Rev.* 117 (2), 712–757.
- Li, J.F., Yin, C.X., Huo, F.J., 2016. Development of fluorescent zinc chemosensors based on various fluorophores and their applications in zinc recognition. *Dyes Pigments* 131, 100–133.
- Linhares, M., Rebelo, S.L.H., Simões, M.M.Q., Silva, A.M.S., Neves, M.G.P.M.S., Cavaleiro, J.A.S., Freire, C., 2014. Biomimetic oxidation of indole by Mn(III)porphyrins. *Appl. Catal. A* 470, 427–433.
- Malinovskii, V.L., Vodzinskii, S.V., Zhilina, Z., Andronati, S.A., Mazepa, A.V., 1996. *Zh. Org. Khim.* 32, 119–123.
- McKenzie, L.K., Bryant, H.E., Weinstein, J.A., 2019. Transition metal complexes as photosensitisers in one- and two-photon photodynamic therapy. *Coord. Chem. Rev.* 379, 2–29.
- Mesquita, M.Q., Dias, C.J., Neves, M., Almeida, A., Faustino, M.A.F., 2018. Revisiting current photoactive materials for antimicrobial photodynamic therapy. *Molecules* 23 (10), 47.
- Moura, N.M.M., Núñez, C., Santos, S.M., Faustino, M.A.F., Cavaleiro, J.A.S., Almeida Paz, F.A., Neves, M.G.P.S., Capelo, J.L., Lodeiro, C., 2014a. A new 3,5-bisporphyrinylpyridine derivative as a fluorescent ratiometric probe for zinc ions. *Chem. Eur. J.* 20 (22), 6684–6692.
- Moura, N.M.M., Núñez, C., Santos, S.M., Faustino, M.A.F., Cavaleiro, J.A.S., Neves, M.G.P.M.S., Capelo, J.L., Lodeiro, C., 2014b. Synthesis, spectroscopy studies, and theoretical calculations of new fluorescent probes based on pyrazole containing porphyrins for Zn(II), Cd(II), and Hg(II) optical detection. *Inorg. Chem.* 53 (12), 6149–6158.
- Moura, N.M.M., Ramos, C.I.V., Linhares, I., Santos, S.M., Faustino, M.A.F., Almeida, A., Cavaleiro, J.A.S., Amado, F.M.L., Lodeiro, C., Neves, M.G.P.M.S., 2016. Synthesis, characterization and biological evaluation of cationic porphyrin-terpyridine derivatives. *RSC Adv.* 6 (112), 110674–110685.
- Mukhopadhyay, R.D., Kim, Y., Koo, J., Kim, K., 2018. Porphyrin boxes. *Acc. Chem. Res.* 51 (11), 2730–2738.
- Nakagaki, S., Mantovani, K., Sippel Machado, G., de Freitas, Dias, Castro, K., Wypych, F., 2016. Recent advances in solid catalysts obtained by metalloporphyrins immobilization on layered anionic exchangers: a short review and some new catalytic results. *Molecules* 21 (3), 291.
- Neves, C.M.B., Filipe, O.M.S., Mota, N., Santos, S.A.O., Silvestre, A. J.D., Santos, E.B.H., Neves, M.G.P.S., Simões, M.M.Q., 2019. Photodegradation of metoprolol using a porphyrin as photosensitizer under homogeneous and heterogeneous conditions. *J. Hazard. Mater.* 370, 13–23.
- Niu, T., Li, A., 2013. Exploring single molecules by scanning probe microscopy: porphyrin and phthalocyanine. *J. Phys. Chem. Lett.* 4 (23), 4095–4102.
- Ostrowski, S., Urbańska, N., Mikus, A., 2003. Nucleophilic substitution of hydrogen in meso-nitroaryl-substituted porphyrins—unprotected at the NH-centers in the core ring. *Tetrahedron Lett.* 44 (23), 4373–4377.
- Ostrowski, S., Mikus, A., Łopuszyńska, B., 2004. Synthesis of highly substituted meso-tetraarylporphyrins. *Tetrahedron* 60 (51), 11951–11957.
- Ostrowski, S., Raczko, A.M., 2005. Selective double functionalization of meso-tetraphenylporphyrin complexes on the same pyrrole unit by tandem electrophilic/nucleophilic aromatic substitution. *Helv. Chim. Acta* 88 (5), 974–978.
- Ostrowski, S., Kosmalka, M., Mikus, A., 2017. A vicarious approach to porphyrin aldehydes. *Tetrahedron Lett.* 58 (21), 2011–2013.
- Otsuki, J., 2018. Supramolecular approach towards light-harvesting materials based on porphyrins and chlorophylls. *J. Mater. Chem. A* 6 (16), 6710–6753.
- Paolesse, R., Nardis, S., Monti, D., Stefanelli, M., Di Natale, C., 2017. Porphyrinoids for chemical sensor applications. *Chem. Rev.* 117 (4), 2517–2583.
- Pegis, M.L., Wise, C.F., Martin, D.J., Mayer, J.M., 2018. Oxygen reduction by homogeneous molecular catalysts and electrocatalysts. *Chem. Rev.* 118 (5), 2340–2391.
- Pereira, A.M.V.M., Alonso, C.M.A., Neves, M.G.P.M.S., Tomé, A. C., Silva, A.M.S., Paz, F.A.A., Cavaleiro, J.A.S., 2008. A new synthetic approach to N-arylquinolino[2,3,4-at]porphyrins from  $\beta$ -arylaminoporphyryns. *J. Org. Chem.* 73 (18), 7353–7356.
- Pereira, A.M.V.M., Cerqueira, A.F.R., Moura, N.M.M., Iglesias, B. A., Faustino, M.A.F., Neves, M.G.P.M.S., Cavaleiro, J.A.S., Lima, M.J.C., da Cunha, A.F., 2014.  $\beta$ -(p-Carboxyaminophenyl)-

- porphyrin derivatives: new dyes for TiO<sub>2</sub> dye-sensitized solar cells. *J. Nanopart. Res.* 16 (11), 2647.
- Radi, S., Abiad, C.E., Moura, N.M.M., Faustino, M.A.F., Neves, M. G.P.M.S., 2019. New hybrid adsorbent based on porphyrin functionalized silica for heavy metals removal: synthesis, characterization, isotherms, kinetics and thermodynamics studies. *J. Hazard. Mater.* 370, 80–90.
- Rajora, M.A., Lou, J.W.H., Zheng, G., 2017. Advancing porphyrin's biomedical utility via supramolecular chemistry. *Chem. Soc. Rev.* 46 (21), 6433–6469.
- Ramos, C.I.V., Graça Santana-Marques, M., Ferrer-Correia, A.J., Barata, J.F.B., Tomé, A.C., Neves, M.G.P.M.S., Cavaleiro, J.A.S., Abreu, P.E., Pereira, M.M., Pais, A.A.C.C., 2012. Differentiation of aminomethyl corrole isomers by mass spectrometry. *J. Mass Spectrom.* 47 (4), 516–522.
- Ramos, C.I.V., Pereira, P.M.R., Santana-Marques, M.G., De Paula, R., Simões, M.M.Q., Neves, M.G.P.M.S., Cavaleiro, J.A.S., 2014. Imidazole and imidazolium porphyrins: gas-phase chemistry of multicharged ions. *J. Mass Spectrom.* 49 (5), 371–379.
- Ramos, C.I.V., Moura, N.M.M., Santos, S.M.F., Faustino, M.A., Tomé, J.P.C., Amado, F.M.L., Neves, M.G.P.M.S., 2015. An insight into the gas-phase fragmentations of potential molecular sensors with porphyrin-chalcone structures. *Int. J. Mass Spectrom.* 392, 164–172.
- Ramos, C.I.V., Figueira, F., Polêto, M.D., Amado, F.M., Verli, H., Tomé, J.P.C., Neves, M.G.P., 2016. ESI-MS/MS of expanded porphyrins: a look into their structure and aromaticity. *J. Mass Spectrom.* 51 (5), 342–349.
- Rebello, S.L.H., Simões, M.M.Q., Neves, M.G.P.M.S., Silva, A.M.S., Cavaleiro, J.A.S., 2004. An efficient approach for aromatic epoxidation using hydrogen peroxide and Mn(III) porphyrins. *Chem. Commun.* 5, 608–609.
- Rebello, S.L.H., Simões, M.M.Q., Neves, M.G.P.M.S., Silva, A.M.S., Tagliatesta, P., Cavaleiro, J.A.S., 2005. Oxidation of bicyclic arenes with hydrogen peroxide catalysed by Mn(III) porphyrins. *J. Mol. Catal. A: Chem.* 232 (1), 135–142.
- Rebello, S.L.H., Gonçalves, A.R., Pereira, M.M., Simões, M.M.Q., Neves, M.G.P.M.S., Cavaleiro, J.A.S., 2006. Epoxidation reactions with hydrogen peroxide activated by a novel heterogeneous metalloporphyrin catalyst. *J. Mol. Catal. A: Chem.* 256 (1), 321–323.
- Richeter, S., Hadj-Aïssa, A., Taffin, C., van der Lee, A., Leclercq, D., 2007. Synthesis and structural characterisation of the first N-heterocyclic carbene ligand fused to a porphyrin. *Chem. Commun.* 21, 2148–2150.
- Saegusa, Y., Ishizuka, T., Komamura, K., Shimizu, S., Kotani, H., Kobayashi, N., Kojima, T., 2015. Ring-fused porphyrins: extension of  $\pi$ -conjugation significantly affects the aromaticity and optical properties of the porphyrin  $\pi$ -systems and the Lewis acidity of the central metal ions. *Phys. Chem. Chem. Phys.* 17, 15001–15011.
- Sandland, J., Malatesti, N., Boyle, R., 2018. Porphyrins and related macrocycles: combining photosensitization with radio- or optical-imaging for next generation theranostic agents. *Photodiagn. Photodyn. Ther.* 23, 281–294.
- Serra, V.I.V., Pires, S.M.G., Alonso, C.M.A., Neves, M.G.P.M.S., Tomé, A.C., Cavaleiro, J.A.S., 2014. Meso-tetraarylporphyrins bearing nitro or amino groups: synthetic strategies and reactivity profiles. In: Paolesse, R. (Ed.), *Synthesis and Modifications of Porphyrinoids*. Springer, Berlin Heidelberg, Berlin, Heidelberg, pp. 35–78.
- Silva, E.M.P., Domingues, M.R.M., Barros, C., Faustino, M.A.F., Tomé, J.P.C., Neves, M.G.P.M.S., Tomé, A.C., Santana-Marques, M.G., Cavaleiro, J.A.S., Ferrer-Correia, A.J., 2005. Characterization of dinitroporphyrin zinc complexes by electrospray ionization tandem mass spectrometry. unusual fragmentations of  $\beta$ -(1,3-dinitroalkyl) porphyrins. *J. Mass Spectrom.* 40 (1), 117–122.
- Soares, A.R.M., Martínez-Díaz, M.V., Bruckner, A., Pereira, A.M.V. M., Tomé, J.P.C., Alonso, C.M.A., Faustino, M.A.F., Neves, M. G.P.M.S., Tomé, A.C., Silva, A.M.S., Cavaleiro, J.A.S., Torres, T., Guldi, D.M., 2007. Synthesis of novel N-linked porphyrin–phthalocyanine dyads. *Org. Lett.* 9 (8), 1557–1560.
- Song, H., Liu, Q., Xie, Y., 2018. Porphyrin-sensitized solar cells: systematic molecular optimization, coadsorption and cosensitization. *Chem. Commun.* 54, 1811–1824.
- Tabolin, A.A., Sukhorukov, A.Y., Ioffe, S.L., Dilman, A.D., 2017. Recent advances in the synthesis and chemistry of nitronates. *Synthesis* 49 (15), 3255–3268.
- Thomas, K.E., Conradie, J., Beavers, C.M., Ghosh, A., 2020. Free-base porphyrins with localized NH protons. Can substituents alone stabilize the elusive cis tautomer?. *Org. Biomol. Chem.* <https://doi.org/10.1039/d0ob00452a> (Advance Article).
- Urbani, M., Grätzel, M., Nazeeruddin, M.K., Torres, T., 2014. Meso-substituted porphyrins for dye-sensitized solar cells. *Chem. Rev.* 114 (24), 12330–12396.
- Vale, L.S.H.P., Barata, J.F.B., Neves, M.G.P.M.S., Faustino, M.A.F., Tomé, A.C., Silva, A.M.S., Paz, F.A.A., Cavaleiro, J.A.S., 2007. Novel quinone-fused corroles. *Tetrahedron Lett.* 48 (50), 8904–8908.
- Vamsi, K.N., Suman, K.J.V., Madoori, M., Seelam, P., Lingamallu, G., 2017. Role of co-sensitizers in dye-sensitized solar cells. *ChemSusChem* 10 (23), 4668–4689.
- Zhang, W., Lai, W., Cao, R., 2017. Energy-related small molecule activation reactions: oxygen reduction and hydrogen and oxygen evolution reactions catalyzed by porphyrin- and corrole-based systems. *Chem. Rev.* 117 (4), 3717–3797.
- Zheng, Z., Ayhan, M.M., Liao, Y.-Y., Calin, N., Bucher, C., Andraud, C., Bretonnière, Y., 2018. Design of two-photon absorbing fluorophores for FRET antenna-core oxygen probes. *New J. Chem.* 42 (10), 7914–7930.